POLITECNICO DI TORINO

Master Course in Aeromechanics and System Engineering

Master Thesis

Design and Development of Optical Sensors Based on FBGs Technology

Supervisor:
Prof. Paolo Maggiore
Co-supervisor:
Ing. Matteo Dalla Vedova

Candidate:
Riccardo Raballo

April 2020

Abstract

Digital sensors are widely adopted in aerospace applications to measure different physical quantities such as temperature, strain and vibration. Despite the high level of fidelity of such sensors they present some disadvantages if compared with some new state-of-the-art technologies. In this work of thesis are presented and tested a new typology of fibre optic sensor: The Fibre Bragg Grating (FBG). One of the most important advantage of these sensors is that it is possible to install many FBGs along one same optical fibre. Moreover, they are lighter and smaller than the traditional ones, they don't need a direct power supply and they are immune to electromagnetic interference as well as to harsh environment. In the future, they are expected to be adopted for prognostic and diagnostic applications in the aerospace sector.
The work has been developed at the Department of Mechanical and Aerospace Engineering (DIMEAS) of Politecnico di Torino in collaboration with the interdepartmental centre Photonext, the Istituto Superiore Mario Boella (ISMB) and Scuola Camerana of Turin.
The objectives of this thesis are to set up a test bench and to test the FBG such as vibration sensor and compare the measurements with the ones provided by a typical accelerometer.
The test bench has been produced by Scuola Camerana of Turin and all the electronics and brushless motor have been supplied by Siemens.
The FBG sensor has been designed to be tested on the top of a bearing support of a rotating shaft that can generate vibration thanks to a rotating wheel on which can be mounted an eccentric mass.
Part of this work is focused on the test bench setting, on the parameter's definition for motion law of the electric motor and especially on the design of FBGs PLA supports printed in 3D. Finally, some tests are carried out measuring the vibration on the top of a mechanical shaker with the FBG sensor to verify the effectiveness so that in the future will be possible to compare the results obtained by tests on the rotating unbalanced shaft with the output of a Siemens accelerometer. In the end, to complete the study of the support, has been carried out a dynamic simulation to find out when to expect amplifications due to the resonance of the support.
The results show how this FBG sensors designed for the vibration test bench is ready to be tested and coming soon the next-generation-sensor in future aerospace applications.

Sommario

I sensori digitali sono ampiamente utilizzati nelle applicazioni aerospaziali per misurare diverse quantità fisiche come temperatura, deformazione e vibrazioni. Nonostante l'elevato livello di fedeltà di tali sensori, essi presentano alcuni svantaggi rispetto ad alcune nuove tecnologie all'avanguardia. In questo lavoro di tesi vengono presentate e testate una nuova tipologia di sensore a fibra ottica: The Fiber Bragg Grating (FBG). Uno dei vantaggi più importanti di questi sensori è che è possibile installare molti FBG su una stessa fibra ottica. Inoltre, sono più leggeri e più piccoli di quelli tradizionali, non hanno bisogno di un alimentazione diretta e sono immuni da interferenze elettromagnetiche e da ambienti corrosivi. In futuro, dovrebbero essere adottati per applicazioni prognostiche e diagnostiche nel settore aerospaziale.
Il lavoro è stato sviluppato presso il Dipartimento di Ingegneria Meccanica e Aerospaziale (DIMEAS) del Politecnico di Torino in collaborazione con il centro interdipartimentale Photonext, l'Istituto Superiore Mario Boella (ISMB) e la Scuola Camerana di Torino.
Gli obiettivi di questa tesi sono di istituire un banco di prova e testare FBG come un sensore di vibrazione e confrontare le misurazioni con quelle fornite da un tipico accelerometro.
Il banco prova è stato prodotto dalla Scuola Camerana di Torino e tutta l'elettronica e il motore brushless sono stati forniti da Siemens.
Il sensore FBG è stato progettato per essere testato sulla parte superiore di un supporto cuscinetto di un albero rotante che può generare vibrazioni grazie a una ruota rotante su cui può essere montata una massa eccentrica.
Parte di questo lavoro si concentra sull'impostazione del banco prova, sulla definizione dei parametri per la legge di moto del motore elettrico e in particolare sulla progettazione del supporto del FBG stampato in 3D. Infine, vengono eseguiti alcuni test misurando la vibrazione su uno shaker meccanico con il sensore FBG per verificarne l'efficacia in modo che in futuro sarà possibile confrontare i risultati ottenuti dai test sull'albero sbilanciato rotante con l'output dell’accelerometro Siemens. Alla fine, per completare lo studio del supporto, è stata effettuata una simulazione dinamica per scoprire quando aspettarsi amplificazioni dovute alla risonanza dello stesso.
I risultati mostrano come questo sensore FBG progettato per il banco di prova a vibrazione è pronto per essere testato e presto questa tecnologia potrà essere adottata nella sensoristica di prossima generazione nelle future applicazioni aerospaziali.

Contents

List of figures

Chapter 1: Introduction

Mechanical vibration is the vibration that can be sensed and measured on the surface of objects. When dealing with machine monitoring, this especially includes the surfaces of machines, components and foundations.
Mechanical vibration is propagated in solid structures and always occurs when mass moves. Such mass may be rotating or oscillating parts of machines and it can be generated also when gasses or fluids collide with solid objects. When dealing with machine diagnostic mechanical vibration has an especially high information content in several respects as:

- Indication of the machine condition;
- Indication of dynamic stresses on the machine, machine base, adjacent machine components;
- Indication of safety of operation, service life, and economic efficiency of machines;
- Basics of machine diagnostics and vibration damping.

Nowadays, the most common way of measuring vibrations is the use of piezoelectric acceleration sensors (accelerometer) that are used for the frequencies and frequency bands to be covered for vibration monitoring. These sensors generate an analog voltage signal that can be further processed in response to dynamic compressive and tensile forces [1]. To this regard, figure 1 shows an example of an accelerometer sensor with the characteristic frequency response.

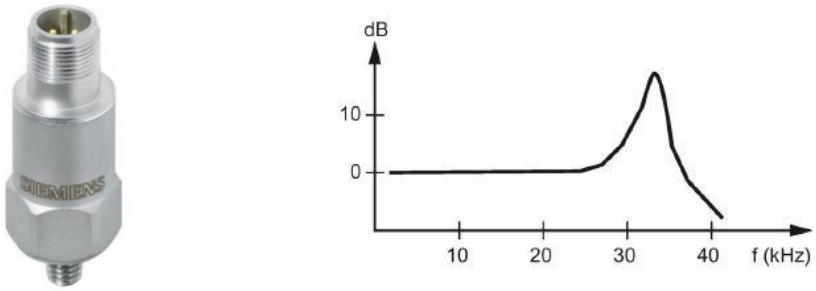

FIGURE 1: AN ACCELEROMETER AND ITS TYPICAL RESPONSE

However, thanks to technology improvements of the latest years, new solutions have been developed in the field of sensors to better overcome some of the limitations of the traditional sensors. One of the most interesting innovations, subject of this thesis, are optical fibre sensors which will probably replace the traditional ones in future aerospace and industrial applications. These types of sensors are simply sections of treated optical fibre that are located along an optical fibre, called Fibre Bragg Grating or FBG.
Compared to their electrical counterparts, sensors within optical fibres have fundamental advantages like totally electromagnetic immunity. Most importantly, one can interrogate lots of sensors within a single optical fibre at arbitrary locations along both great and minimal distances, besides of being as thin as a human hair, weighing next to nothing, and running robustly at high temperatures or even in highly corrosive and high radiation environments [2].

Chapter 2: Optical Fibres

2.1 General Description and Classification

Optical glass fibres are optical devices made of glass or polymeric materials that exploit the ability to transmit information over great distances thanks to the light that runs inside them. They are widely used in telecommunication sector as data transportation system driving the light with minimal signal attenuation and exploiting the total reflection principle. The ability to transmit the light is expressed by the refractive index:

$$n = \frac{c}{v}$$

Where c is the speed of light in vacuum and v is the speed of light inside the considered material. Optical fibres are typically composed by silicon dioxide (SiO2) which refractive index is n = 1.5 meaning that the light travels inside the fibre at 2/3 of the speed of light in vacuum.

As shown in figure 2, the general structure of an optical fibre is composed by three elements:

- Core
- Cladding
- Coating

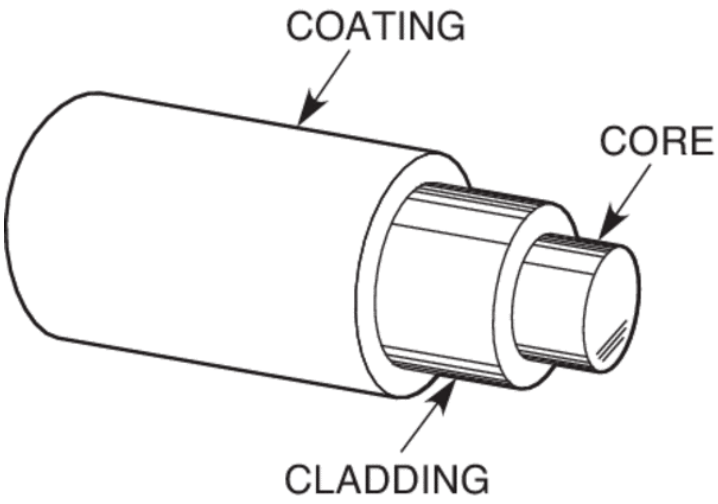

FIGURE 2: OPTICAL FIBRE'S STRUCTURE

The core is the inner layer where occurs the total internal reflection (TIR) phenomenon caused by the different refractive index of the surrounding layer called cladding, this allows the light to be confined within the core. The core has variable dimensions from 8 μm to 62.5 μm.

The external coating is the layer that protects the inner layers and provides mechanical resistance to the entire structure.

The light propagates as electromagnetic wave within the fibre having different paths and geometries that represent different propagation modes of the fibre. Each propagation

mode is identified with the mode *m = 0, 1, 2, etc.* and has a different propagation velocity. It's possible, optimizing the fibre's parameters, to allow only the propagation of the fundamental mode (m=0), this kind of optical fibres are single mode ones.
So, it is possible to classify the optical fibres according to the light's propagation mode and refractive indexes inside them:

- *Step-index single mode fibre*: is a kind of fibre used only with laser sources for long distances applications in which low signal loss and high data rates are required. The light travels along the fibre without reflections according to the fundamental mode (m=0), this allows to provide a higher bandwidth than the multimode fibres because the reflections generate a modal dispersion that limits the bandwidth.
- *Step-index multimode fibre*: is a fibre in which is permitted to have many propagation modes because of the large core diameter characterized by a uniform index of reflection. The name step-index is because of the different refractive index of the core and the cladding that is slightly lower. Higher order modes propagate along the fibre with lower angles respect to the lower order modes.
- *Graded-index multimode fibre*: this fibre has been developed to avoid modal dispersion that characterize the multimode step-index fibres. This is obtained with a varying core index with the distance from the centre while the value of the cladding refractive index is constant.

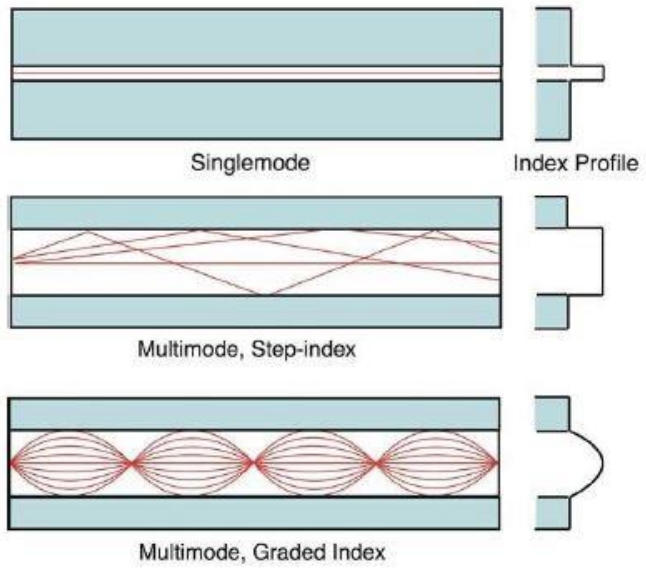

FIGURE 3: DIFFERENT MODES OF PROPAGATION

As shown in figure 3, the light rays of different order in the multimode step-index fibre reach the final position at different times while in the graded index fibre they are forced to reach the same position at the same time, due to the variation of the core refractive index [3].

2.2 Working principle

The propagation of light beams along the fibre is based on the total internal refraction phenomenon described by the theories of the geometric optics. In particular, the Snell's law describes the total internal refraction of light when it passes from a material to another with a different refractive index, allowing the propagation of the light signals. Let's understand the Snell's law introducing the formulation:

$$n_1 sin\theta_i = n_2 sin\theta_t$$

Where:

- n_1 and n_2 are the refractive indexes of the materials
- θ_i is the incident angle of the light ray
- θ_t is the reflected angle of the light ray

Assuming n_1 and n_2 constant, the angle θ_t varies only depending on the incident angle θ_i, as shown in figure 4:

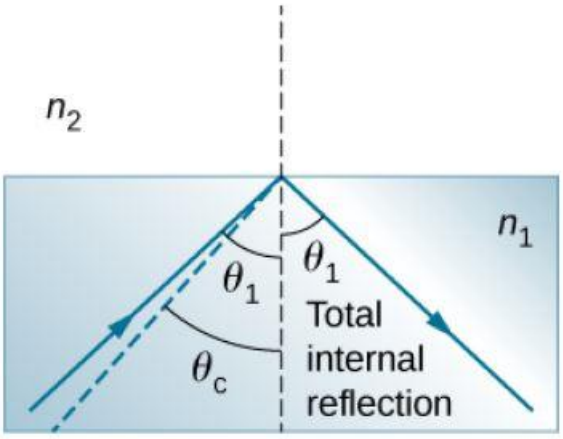

FIGURE 4: TOTAL INTERNAL REFLECTION

The light beam can travel along the fibre until the end only if the angle of incidence is greater than the *critical angle* θ_c , in this case the total refraction phenomenon occurs and there is no loss of signal because the light is confined inside the core.
The *critical angle* θ_c can be found imposing the reflected angle at 90° in the Snell's law:

$$n_1 sin\theta_c = n_2 \sin\frac{\pi}{2}$$

$$\theta_c = arcsin\frac{n_2}{n_1}$$

So, not all the light is guided along the fibre but only the rays that are inside an *acceptance cone*, described by an angle α_{max} with respect to the fibre axis at the entrance of the fibre can propagate, as shown in figure 5 [4]:

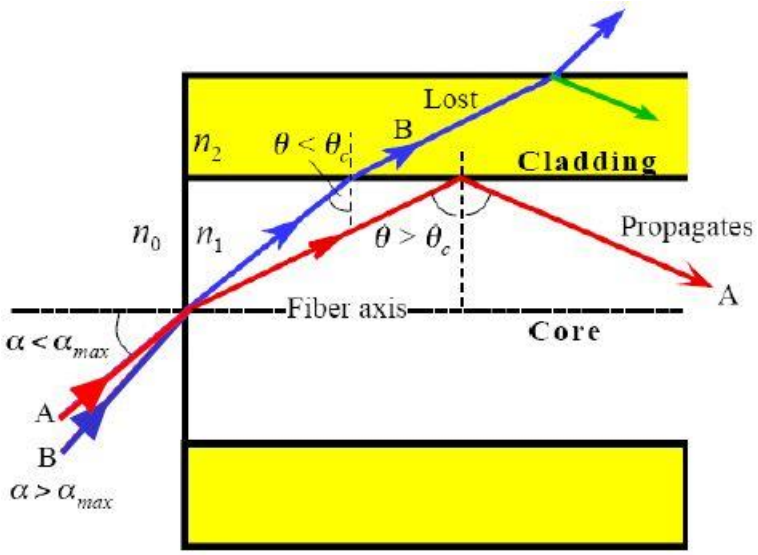

FIGURE 5: ACCEPTAMCE CONE

If the angle $\alpha < \alpha_{max}$ the ray can reach the interface with the cladding with an angle greater than θ_c, allowing the propagation, while if the ray has an incidence angle greater than α_{max} the ray "escapes" in the cladding losing the signal.
Is important to find the exact value of α_{max} that allows the TIR which involves $\theta = \theta_c$, considering the first interface, according to the Snell's law:

$$n_0 sin\alpha = n_1 \sin\left(\frac{\pi}{2} - \theta_c\right)$$

Since θ_c is known, substituting:

$$sin\alpha_{max} = \frac{n_1 cos\theta_c}{n_0} = \frac{n_1}{n_0}\sqrt{1 - sin^2\theta_c} = \frac{(n_1^2 - n_2^2)^{1/2}}{n_0}$$

Where:

$$(n_1^2 - n_2^2)^{1/2} = NA$$

NA is the *numerical aperture*, finally:

$$\alpha_{max} = arcsin\frac{NA}{n_0}$$

2.3 Advantages and Disadvantages

Optical fibres are recently more and more used in many sectors, especially in the telecommunication one but also for many aerospace applications because of the many advantages they have if compared to the traditional copper transmission.
It's possible to summarise some of the of advantages the optical fibres [5]:

- Optical fibres can transfer a very large amount of information thanks to its bandwidth at high speed over long distances because of the very low losses, while transmission with copper has several limitations for distances and bandwidth.
- They are much lighter in weight than copper, flexible, temperature resistant and chemically neutral so they can be applied in extreme environments without the danger of corrosion.
- The materials used to manufacture the fibres, typically glass and plastic, are non-conducting so they have no interaction with electromagnetic fields. They are perfect for aerospace applications since they cannot be affected by other electronic devices or space cosmic radiations.
- They are safe because they don't overheat and don't produce sparkles.
- Glass is more abundant than copper, so they are cheaper also because they are very easy to manufacture and the total costs for production and logistics are decreasing over the years.

Some of the disadvantages of the optical fibres are:

- They are very delicate, so they need a good protection if subjected to mechanical stresses.
- They need to be installed with high curvature radius because of the performance losses and the danger to be broken.
- Installation and equipment used in combination with optical fibre are very expensive. Using FBG sensors requires an expensive interrogation system, also requires expensive equipment to splice two or more optical fibres.

Chapter 3: Optical sensors

As already mentioned, optical fibres are often used for data transmission in the telecommunication sector, but they are finding new applications in the aerospace fields as sensors: indeed, is possible to measure several physical quantities as pressure, stress, strain, temperature, vibration and others.
Such measurements are very important for example in the field of smart structures where sensors have a key role to monitor the conditions and supply the information to the control system that processes it and generate a useful effect, thanks to the actuators, to vary or restore the working conditions.
The main advantage of using optical fibre sensors is that they don't need electrical power to work. Power source is required to the expensive equipment needed to process the measurement, but it can be installed far away from the sensor in remote places.
Optical sensors are integral part of the fibre, so they are very small and light weighted, and it's possible to equip a single fibre with multiple sensors.
In this thesis are used optical sensors named *Fibre Bragg Gratings*, or FBG, which characteristics and working principle, classification and manufacture are explained in the next sections.

3.1 Fibre Bragg Gratings

FBG sensors are basically a wavelength filters made by a periodic variation of the core's refractive index of an optical fibre. When the light passes through a Bragg sensor, only a specific wavelength is reflected to the source, denominated Bragg wavelength λ_B, which correspond to a peak in the reflected spectrum. In figure 6 is possible to notice an FBG structure where n3 is the variation of the core's refractive index [2].

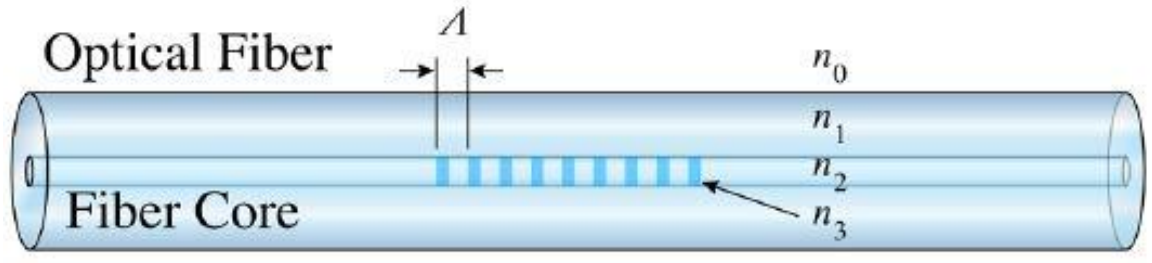

FIGURE 6: FBG STRUCTURE

So, FBG allows only certain frequencies to pass and reflects others, in figure 7 is shown the working principle of a fibre Bragg grating.

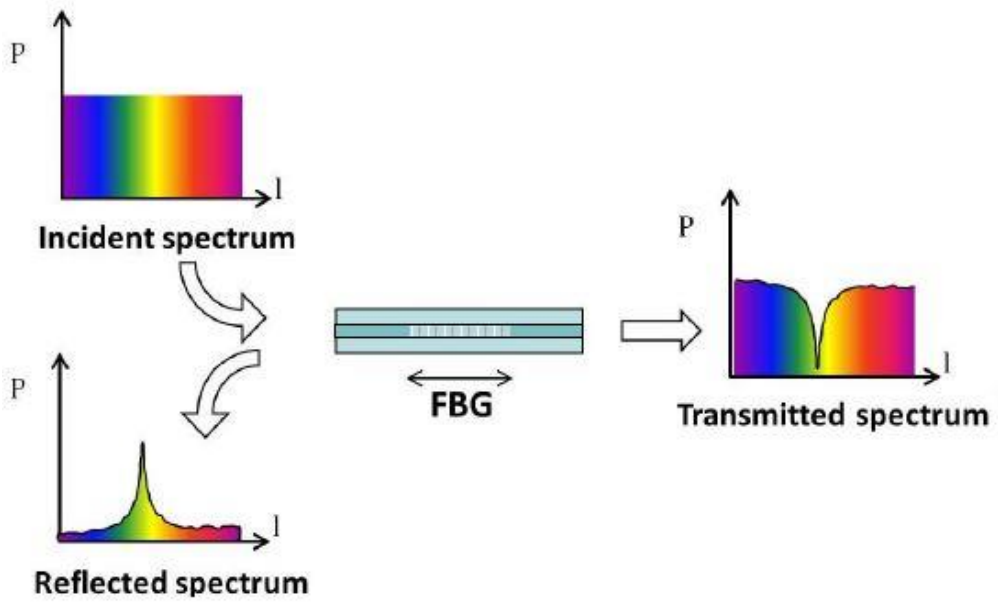

FIGURE 7: FBG WORKING PRINCIPLE

The fundamental equation of the Bragg grating is:

$$\lambda_B = 2 \cdot \eta_{eff} \cdot \Lambda$$

Where:

- $\lambda_B$is the Bragg reflected wavelength;
- η_{eff} is the effective refractive index of the rating's core;
- Λ is the grating period.

However, when external conditions cause the material to expand or compress, the grating step length changes and consequentially the reflected wavelength itself.
So, strain and temperature affect Bragg's reflected wavelength as:

$$\Delta\lambda_B = \Delta\lambda_S + \Delta\lambda_T$$

Where the subscript S show the variation of the reflected wavelength due to the strain, while T for the temperature effect.
Exploiting the term $\Delta\lambda_T$:

$$\Delta\lambda_T = \lambda_B(\alpha + \xi)\Delta T$$

And the term $\Delta\lambda_S$:

$$\Delta\lambda_T = \lambda_B(1 - P_E)\Delta\varepsilon$$

Finally:

$$\Delta\lambda_B = \lambda_B(1 - P_E)\Delta\varepsilon + \lambda_B(\alpha + \xi)\Delta T$$

Where:

- P_E is the photo-elasticity constant.
- $\Delta\varepsilon$ is strain.
- α is the thermal expansion coefficient.

- ξ is the thermo-optic coefficient.
- ΔT is the temperature variation.

The light is emitted by an interrogator as a laser source and the reflected spectrum is analysed as well. This can be visualised in figure 8 where an optical fibre equipped with an FBG is subjected to a strain that causes the elongation.

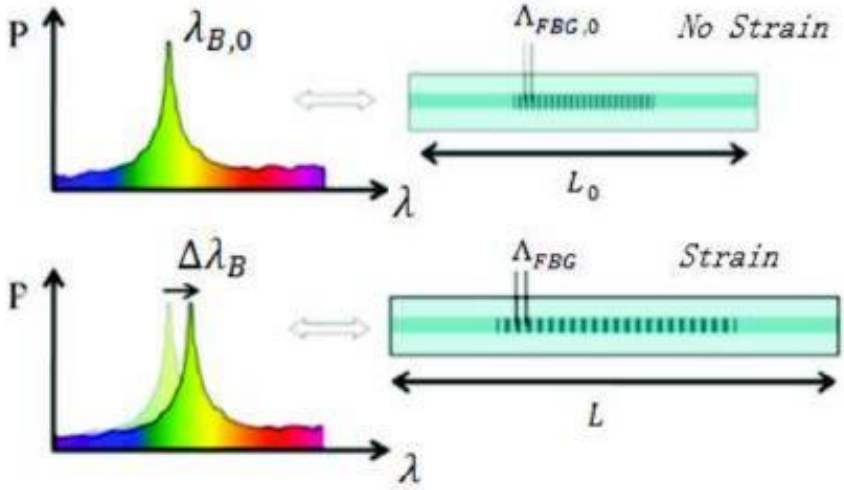

FIGURE 8: WAVELENGTH VARIATION

This kind of sensors are very sensitive: using FBGs as deformation sensors, the field of our interest, is possible to achieve a precision of 0.01 pm on the spectrum which means that deformations in the order of the nano-meter can be detected.

3.2 FBG Classification

In this thesis are used only *short period Bragg gratings* sensors which are different from the *long period Bragg gratings* because of the grating period Λ that is in the order of hundreds of *nm*, while the long period ones have a Λ of fraction of *millimetres*.
Over the years, many short period structures have been developed, modifying the parameter that influence the Bragg wavelength. The parameters to be modified are the period Λ, that is the distance between a part of a treated fibre and one untreated, and the refraction index N.
Here are summarised various types of Bragg gratings [5]:

- *Uniform gratings* are the ones used in this thesis which refractive index follows a harmonic variation, figure 9.

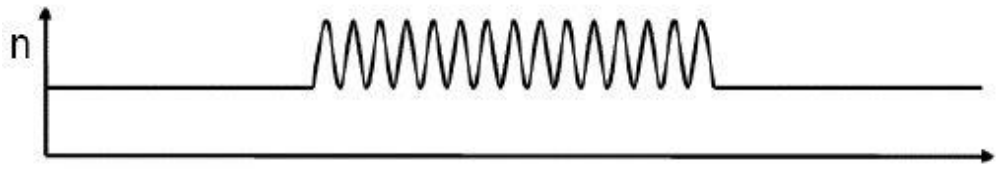

FIGURE 9: UNIFORM GRATING

- *Apodized gratings* are characterised by a narrow bandwidth and suppressed side lobes. The two main shapes of the refractive index that are used are: the Gaussian in figure 10(a) and the cosine one in figure 10(b).

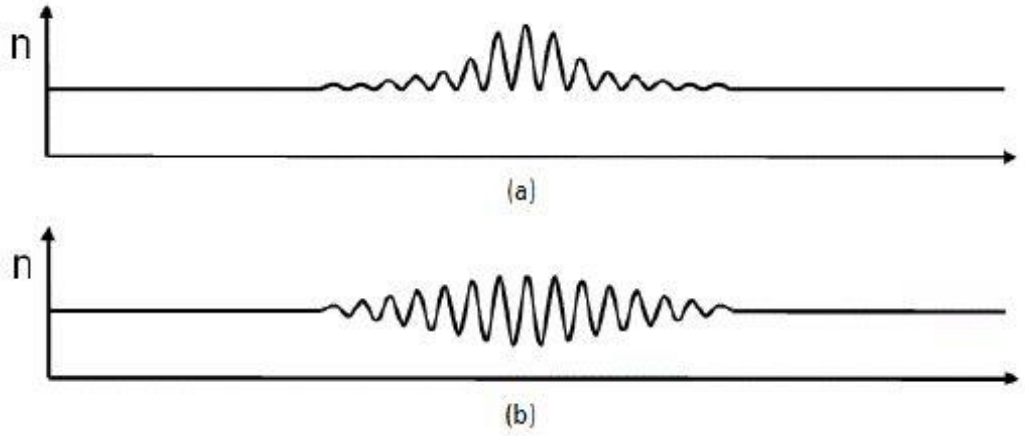

FIGURE 10: APODIZED GRATINGS

- *Phase shifted gratings*, shown in figure 11, have a refractive index where is present a phase shift of π, in the centre of the grating, to modify its reflective spectrum.

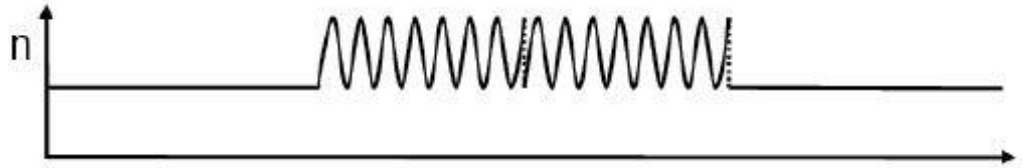

FIGURE 11: PHASE SHIFTED GRATING

- *Chirped Bragg structures* have a grating period Λ modified, typically as a linear variation. This kind of gratings have great resolution and are used to control some type of dispersions. In figure 12 is shown their structure.

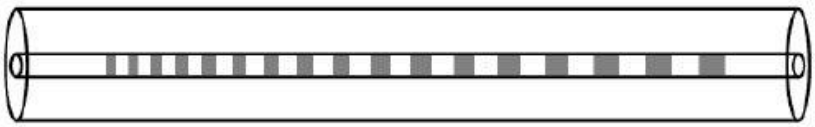

FIGURE 12: CHIRPED BRAGG STRUCTURE

- *Tilted gratings* have a $\Lambda = \text{cost}$ but the peculiarity is that the refractive index n is modulated not normal to the fibre's axe but tilted of an angle ϑ varying from 2° to 20°. The tilting angle ϑ is obtained during the manufacturing process and is needed to control the spectral profile of the grating. An example of the tilted grating is shown in figure 13.

FIGURE 13: TILTED GRATINGS

3.3 FBG manufacture

FBGs sensors are manufactured inside the core of an optical fibre exploiting the property that allows the inscription of the grating, called *photosensivity*. Indeed, if the core is exposed to an intense ultraviolet source of a certain wavelength is possible to change permanently the refractive index and so the characteristics of the grating like the wavelength reflected.
This happens because UV rays damage the fibre's core at atomic level changing its *n* value.
To produce gratings are not used pure silica fibres but germanium-doped fibres that present a better photosensive characteristics.
There are several methods to produce FBGs which the main ones are *Phase-masking, Interfering beams* and *Point by point* method, explained in the following pages [5].

3.3.1 Phase-masking method

The optical fibre is placed under a phase mask that modulates the UV beam with the desired period, as shown in figure 14. The mask surface has a periodic grating which produce an interference pattern on the fibre's core and the Bragg's wavelength of the sensor depends on the phase mask periodicity.
With this technique is possible to produce chirped FBGs, chirping the phase mask, or tilted ones, tilting the mask with an angle of θ.
To build different sensors with a specific Bragg wavelength are needed different phase masks to change in each process and is mandatory to remove the jacket from the optical fibre, making its structure fragile. However, this is the most economical method of production and presents a good repeatability.

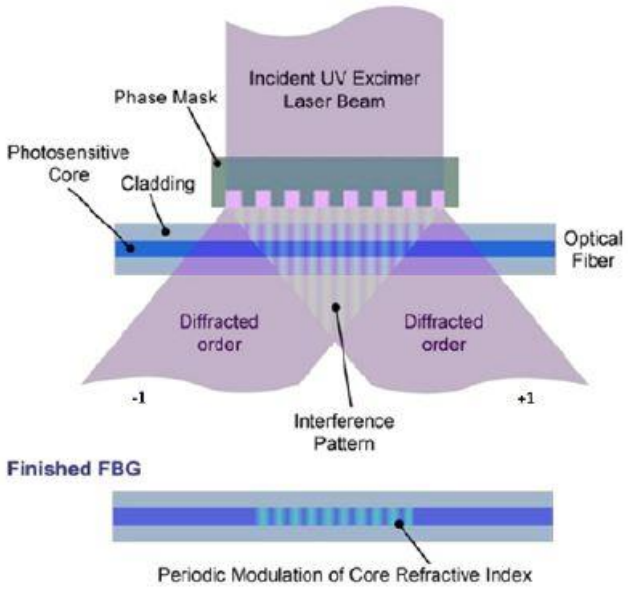

FIGURE 14: PHASE MASKING METHOD

3.3.2 Interfering beams

In this method the UV rays emitted by the source are divided by a splitter and then they reach two orientable mirrors which reflect the rays. The two UV beams are reflected with an angle θ and then are focused, passing through a cylindrical lens, and generate an interference pattern over the fibre to be inscribed, as shown in figure 15. It is necessary to achieve a very high precision during the process to obtain a good result, because the light beams need to perfectly focus with a specific angle over the fibre's core. Moreover, the refractive index variation is directly proportional to the intensity of light emitted by the source. Like the phase-making method the jacket has to be removed during the process, but it is possible to create any Λ value for the interference pattern depending on the wavelength of the laser light source (λ_{laser}) and the angle θ. Indeed, the period Λ is defined by:

$$\Lambda = \frac{(\lambda_{laser})}{2sin\theta}$$

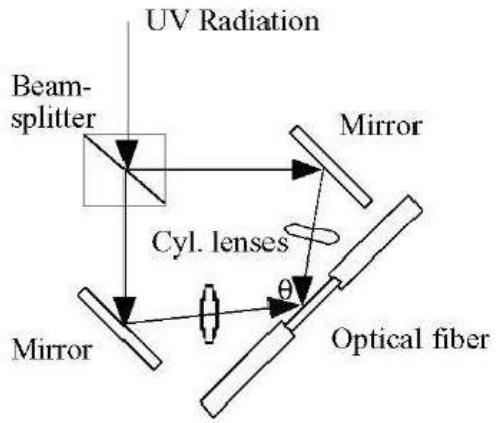

FIGURE 15: INTERFERING BEAMS METHOD

3.3.3 Point by point

In this method high energy impulses are focused over the fibre's core with high precision to inscribe the grating moving the fibre of the quantity Λ at each step. These fast, high energy beams are generated by the focused femtosecond laser system (FLS) and the movement of the fibre requires a very precise control. The main advantage is the possibility to produce FBGs without removing the fibre's jacket but, in the other hand, it is a slow process. Figure 16.

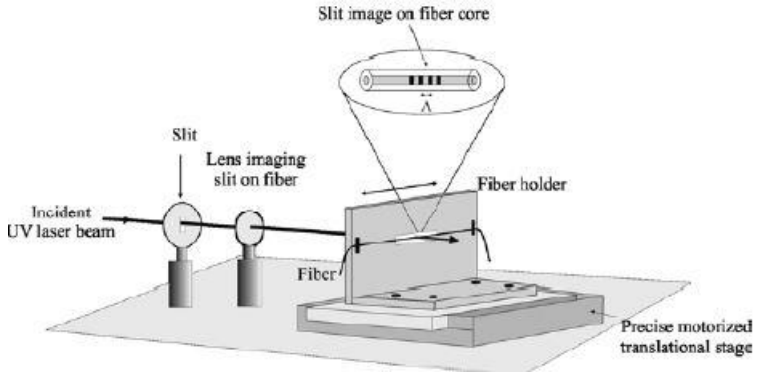

FIGURE 16: POINT BY POINT METHOD

Chapter 4: Test Bench

Mechanical vibration is vibration that can be sensed and measured on the surface of objects. When dealing with machine monitoring, this especially includes the surfaces of machines, components and foundations. In order to conduct the dynamic analysis of the fibre is necessary a set of tools both to provide the motion to the fibre and to retrieve the information about the deformation to which the FBG is subjected to evaluate the mechanical vibration of the machine. The aim of this thesis is design a FBG sensor to measure the vibrations on a rotating shaft that drives a vibration generating wheel. All the mechanical parts such the platform, bearing and accelerometer supports have been produced by Scuola Camerana of Torino.
The shaft is driven by a three-phase brushless motor and is supported by two rotating bearings on which can be mounted both an accelerometer and the FBG sensor on 3D printed PLA support. In this way, the measurements can be compared with the accelerometer supplied by Siemens, that has also provided all the electronics and motor needed for motion. Before testing the FBG sensor on the test bench, some tests have been carried out with different tools, such as a mechanical shaker, in order to find the resonance frequency of the fibre and to confirm the functionality of the sensor.
The measurements are taken by a laser interrogator connected to the fibre that emits and reads the light refracted by the FBG. In this chapter are shown in detail the physical tools used in this thesis.

4.1 Brushless motor and electronics

As already mentioned, the electric motor and the electronics needed for motion have been supplied by Siemens. The shaft is not simply driven by the electric motor powered by electric current but is more complex due to engineering purposes. Indeed, the electric motor is connected to several modules that can be programmed and connected via Ethernet to obtain a desired motion law adjusting the parameters. Moreover, is possible to display and process the vibration measurement from the accelerometer thanks to the SIMATIC HMI touch screen.
The electronic modules of the test bench are:

- Electric breakers;
- Siemens AC/DC converter;
- Siemens PLC;
- Siemens SINAMICS V90 frequency converter;
- Siemens SIMATIC S7-1200 condition monitoring system;
- Siemens SIPLUS CMS2000 VIB sensor (vibration sensor IEPE);
- Siemens SIMATIC HMI touch screen;
- Siemens SCALANCE X ethernet switch;
- Siemens SIMOTICS S-1FL6 brushless motor.

The brushless motor used in this work of thesis is the SIMOTICS S-1FL6 which main features are summarized in table 1:

TABLE 1: ELECTRIC MOTOR SPECIFICATIONS

Measurement and Processing	
Nominal Torque	0.64 Nm
Nominal Power	0.2 kW
Nominal rpm	3000 rpm
Shaft height	30 mm

In the next figures (figure 17 and figure 18) are shown the power and data connections between the electronic modules, note that all the devices are powered in 24 V after the AC/DC conversion from the 230 V AC current.

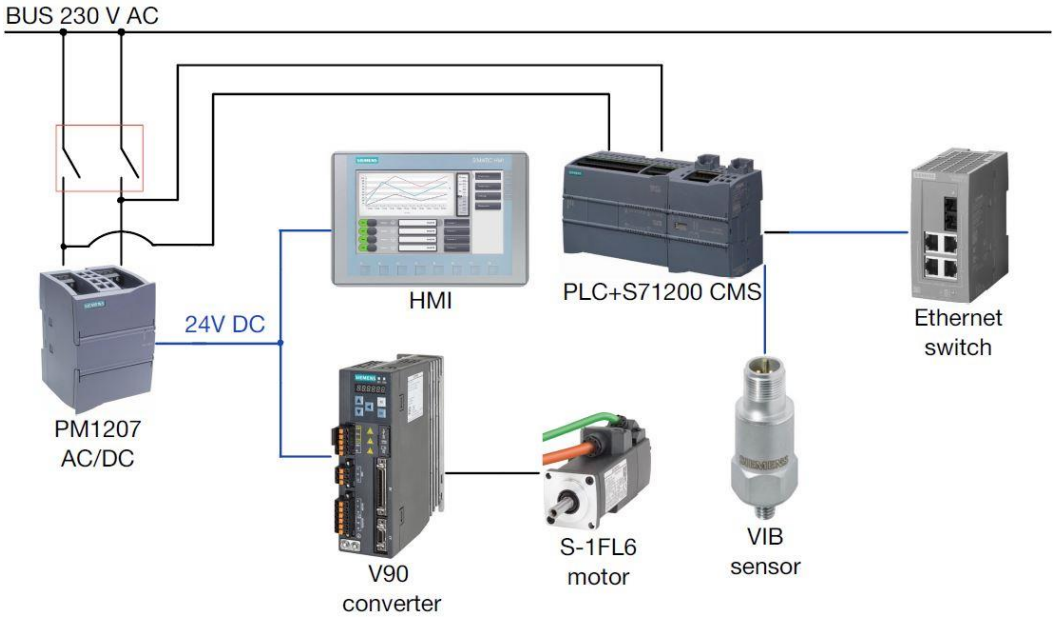

FIGURE 18: ELECTRONICS POWER CONNECTIONS

FIGURE 17: ELECTRONICS DATA CONNECTIONS

4.1.1 Condition Monitoring System

For effective protection of a machine against mechanical damage during operation, the machine should be monitored continuously to detect early signs of such damage. Mechanical vibration is of special significance in this regard. Vibration largely originates from the centrifugal forces on rotating machine parts. Possible causes include:

- Unbalance;
- Misalignment of machine drive trains;
- Bearing damage;
- Gear defect;
- Magnetic, hydraulic and other functional alternating forces.

SIEMENS provides the SIPLUS CMS Condition Monitoring System for the monitoring of mechanical components. With this monitoring system, you can keep an eye on every machine and the entire plant. Maintenance operations can be planned and carried out on schedule and in keeping with the concept of predictive maintenance. After an extended period of fault-free operation, any significant changes resulting from wear and tear or other damage-related causes can be detected at an early stage using the documented trend curves [1]. The Condition Monitoring System uses an accelerometer as vibration sensor to monitor the vibrations on the bearing of the shaft end. In the following figure is shown the configuration of this solution.

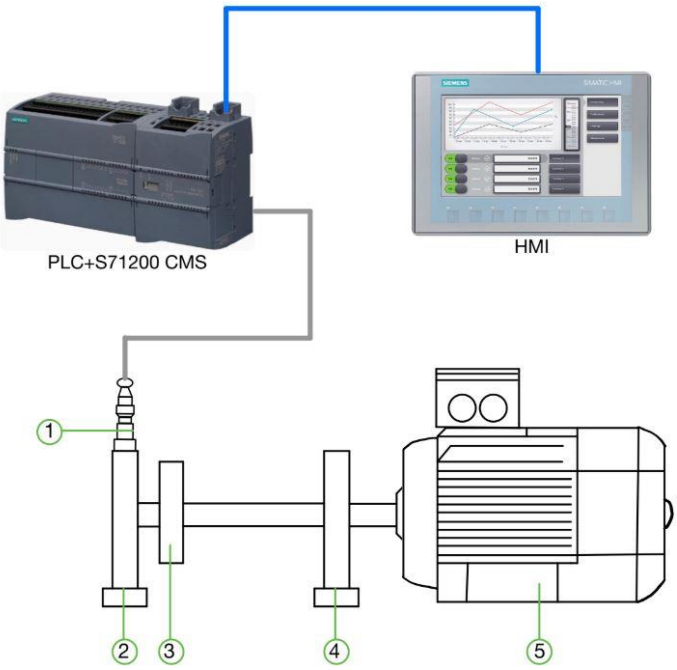

FIGURE 19: CMS CONFIGURATION

TABLE 2: CMS COMPONENTS LEGEND

No.	Description
1	Vibration sensor for detecting the vibration acceleration
2	Bearing at shaft end
3	Load
4	Bearing on the shaft coupling
5	Motor

4.2 Shaft

The shaft used to measure the vibration test is built in aluminium alloy and has been produced in the turning laboratory of Scuola Camerana of Torino.
The mechanical part of the test bench is composed by:

- Platform;
- Siemens brushless motor support;
- Elastic joint, to connect the motor shaft to the main one;
- Two bearing supports with the corresponding bearing;
- The vibration generating wheel, joined to the main shaft between the bearings;
- A plexiglass cover is needed to protect the operator and it is supported by a pneumatic piston to hold the open position.

The wheel has threaded holes along a circumference in which is possible to screw a mass that unbalance the centre of gravity of the wheel in order to generate vibration. The vibration generated are measured by the accelerometer on the top of the bearing support while on the top of the bearing of the shaft end is expected to mount the PLA 3D printed support for the FBG sensor.
In figure 20 is shown the shaft completely assembled.

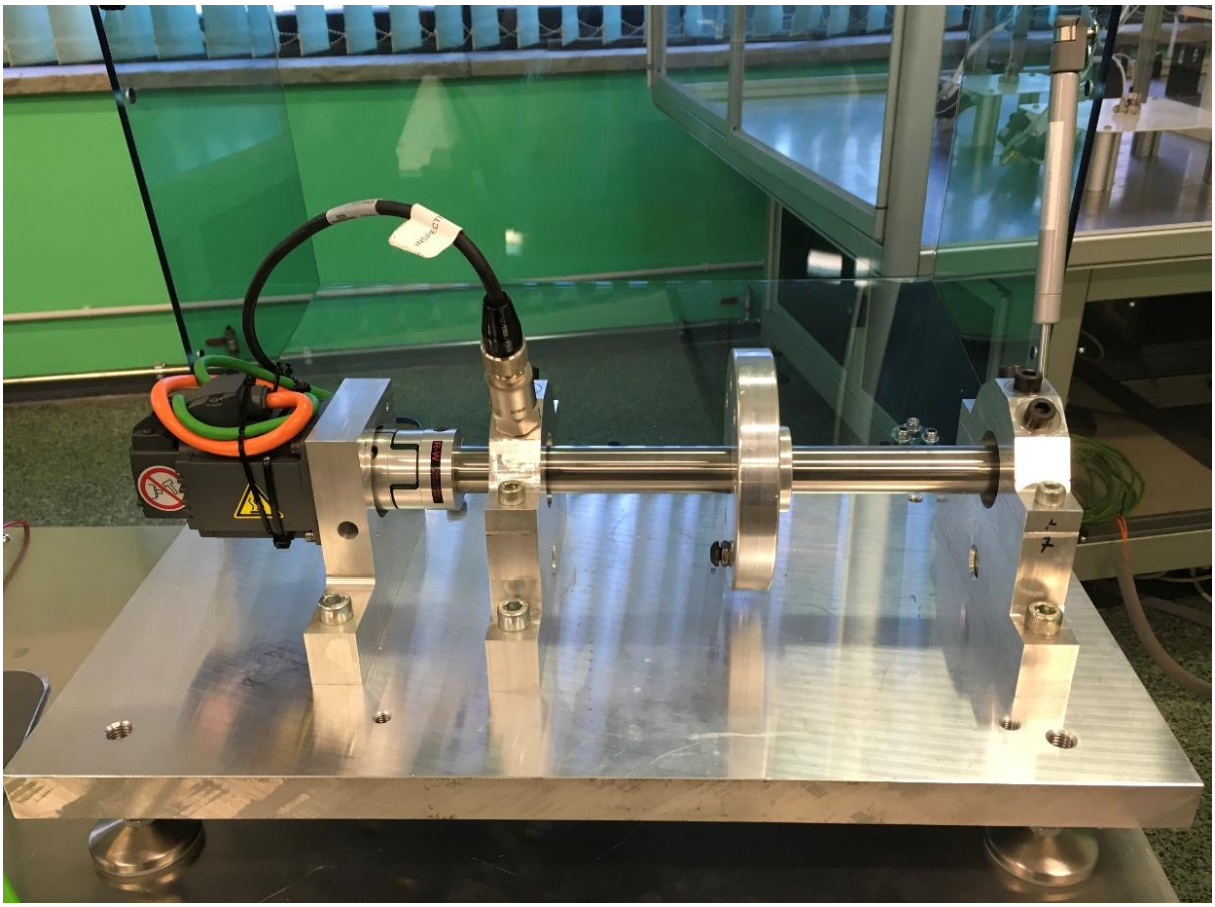

FIGURE 20: SHAFT

4.3 Mechanical shaker

This tool is capable to provide a linear oscillatory motion in the vertical direction and it is necessary to pair the device with:

- Function generator;
- Amplifier.

The function generator can be programmed to obtain a sinusoidal, square, ramp or pulse motion law. For our applications it was used imposing a sinusoidal motion pressing the "SINE" button and varying the frequency with the relative control wheel.
The frequency has been set in Hz and the amplitude in terms of Vpp (peak-to-peak volts).
Through the amplifier is possible to set the gain and a maximum current limit at about 1.5 Ampere. The gain value is useful to change in order to make the oscillations visible or measurable by the sensor without exceeding the current limit, in this case, the system stops automatically. Mechanical shaker, function generator and Amplifier are shown in figure 21.

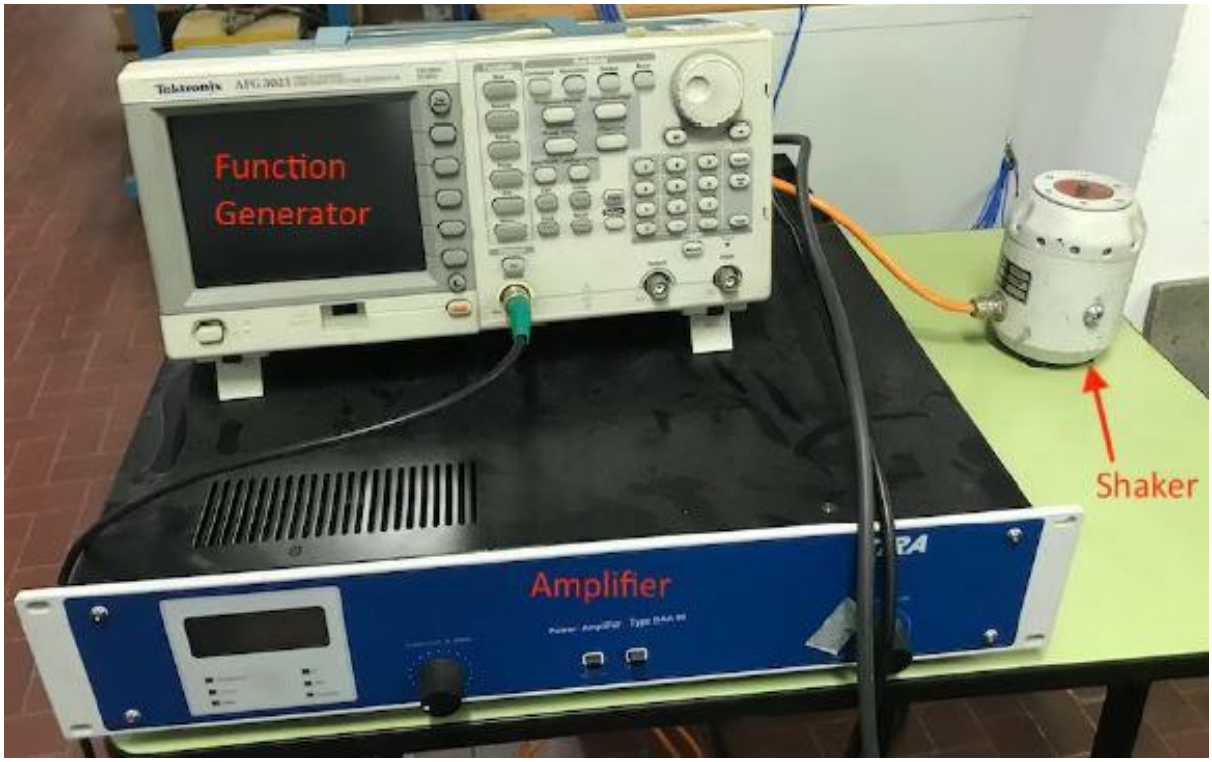

FIGURE 21: MECHANICAL SHAKER, FUNCTION GENERATOR AND AMPLIFIER

4.4 Interrogator

This device is built to acquire the measurements about the behaviours of the fibre thanks to laser beams emitted and reflected by the FBG with a high frequency. The interrogator can be set to acquire several physical measurements such as temperature, strain and pressure analysing the wavelength reflected by the Bragg sensor. The interrogator in use for this thesis is the *SmartFibers SmartScan,* which main specifications are here summarised in table 3:

TABLE 3: INTERROGATOR SPECIFICATIONS

Measurement and Processing	
Wavelength Range	40 nm
N° of optical channels	1,2,3,4
Max N° of sensors	16
Scan frequency (all sensors simultaneously)	2.5 kHz
Max scan frequency (reduced wavelength range)	25 kHz
Dimension	140 x 115 x 85 mm
Weight	0.9 kg

Figure 22 shows the *SmartFibers SmartScan* interrogator.

FIGURE 22: INTERROGATOR

The detailed description of the software will be in the next chapters.

4.5 Micro manual handler

This tool is necessary to pre-tension the optical fibre before gluing it to the 3D printed support. Indeed, as will be explained later, the resonance frequency of the fibre will change if the fibre presents a pre-tension. The pre-tensioning is adopted to change this frequency to avoid this phenomenon in some range of operations. It is a moving support to which the fibre is glued and tensioned by the linear movement of a plate thanks to the rotation of a wheel on the back.
To carry out the micro-strain measurement, the fibre with the FBG is connected to the interrogator and to the PC. The SmartSoft software is used to measure the tensioning, when the desired value is reached the fibre can be glued to the PLA support.

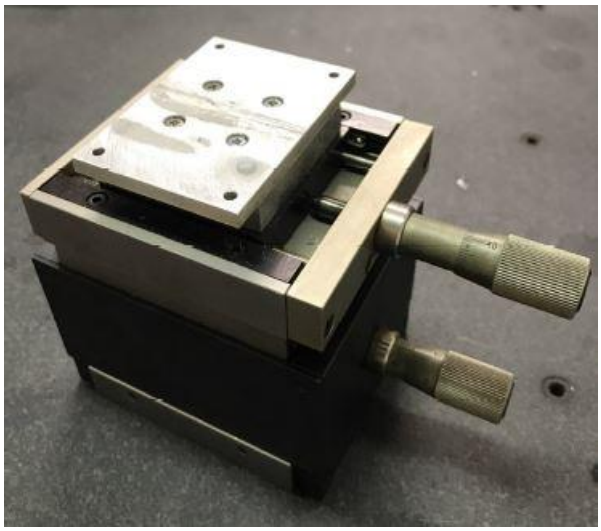

FIGURE 23: MICRO MANUAL HANDLER

4.6 3D printed supports

In order to fix the fibre equipped with the FBG sensor to the test bench, it was necessary to design, and print 3D PLA supports. They were designed using the CAD software *Solidworks Student* and then printed with a 3D printer of Politecnico di Torino. The main advantage to produce a 3D printed support is the relative production speed, in fact, it took just 23 hours to print the first support. Since the test bench is already equipped with a Siemens accelerometer vibration sensor fixed to one of the two bearings supports, the first PLA fibre support was designed to be fixed to the other bearing support in order to compare the vibration measurement obtained during the tests. The bearing support from which our design started is shown in figure 24, and the PLA fibre support is shown in figure 25.

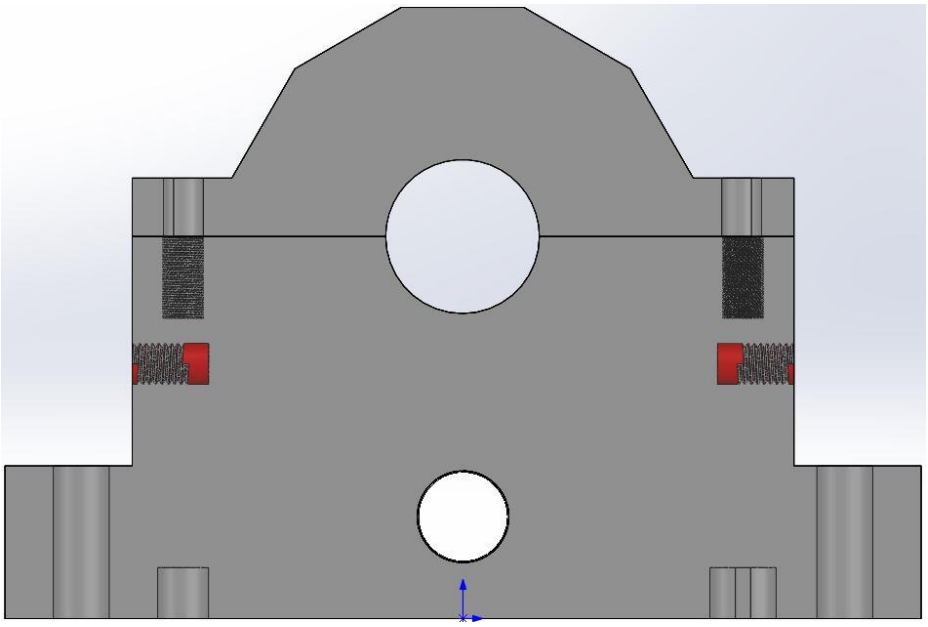

FIGURE 24: BEARING SUPPORT

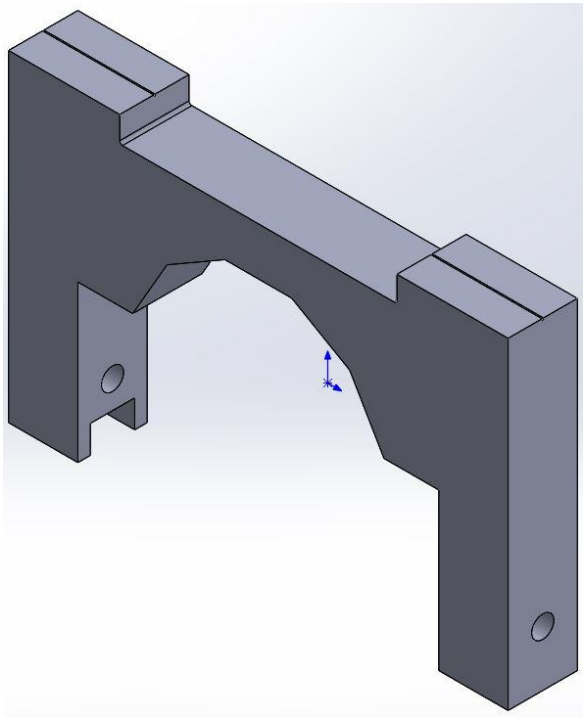

FIGURE 25: PLA FBG SUPPORT

A tolerance of 1 mm was given to the internal distances considering the printing imperfections. The aluminium bearing support has been modified obtaining two threaded holes M8 with a depth of 15 mm to accommodate the screws to fix the support.

Based on previous experience, the fibre has been glued to the fixing points for an adequate length and has also been pre-tensioned to a certain value such as to avoid the resonance of the fibre, as will be detailed in the next chapters. Finally, it has been designed also a cover to protect the fibre from impacts and to double the glued surface of the fibre, shown in figure 26 where is possible to notice the bearing support assembled with the FBG sensor. The 3D printed cover

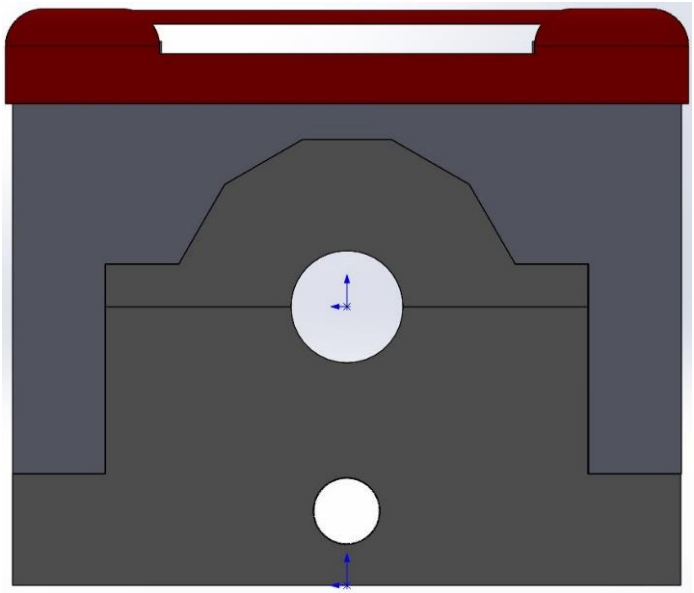

FIGURE 26: FBG SUPPORT ASSEMBLED ON THE BEARING SUPPORT

has been designed with holes on the top and on each side to allow the operator to see the fibre and eventually evaluate when the fibre goes in resonance or if it is damaged.

4.7 Fibre manufacturing tools

To build the fibres equipped with sensors, connectors and coating is necessary a set of tools that are furnished by the Boella laboratory at Politecnico di Torino.
Bragg sensors are supplied already inserted in a section of an optical fibre and then with the splicer is possible to join the fibre to the connector. The re-coater is another tool used to reintroduce the coating that has been removed before the joining of the two fibres. Here are descripted the tools used to create the optical fibres with connectors and sensors.

4.7.1 Cleaver

The specific cleaver shown in figure 27, was used in the laboratory to obtain an almost perfect perpendicular cut of the optical fibre. Before the operation, is needed to remove the external coating with a tweezer and clean the uncovered fibre from residues. The cleaver presents a rotating diamond tip capable to cut the fibre very precisely.

FIGURE 27: CLEAVER

4.7.2 Splicer

The splicer is a tool capable to join two fibres using an electric arc to weld them together. It is necessary to remove the protective sheath from the fibre and the coating that protect the glass core before inserting the fibres in the machine. Moreover, the end of the fibre must be perfectly perpendicular to the fibre axe, this is obtained thanks to the cleaver. When the fibre is ready to be joined with the FBG segment is possible to see the fibre's structure as in figure 28.

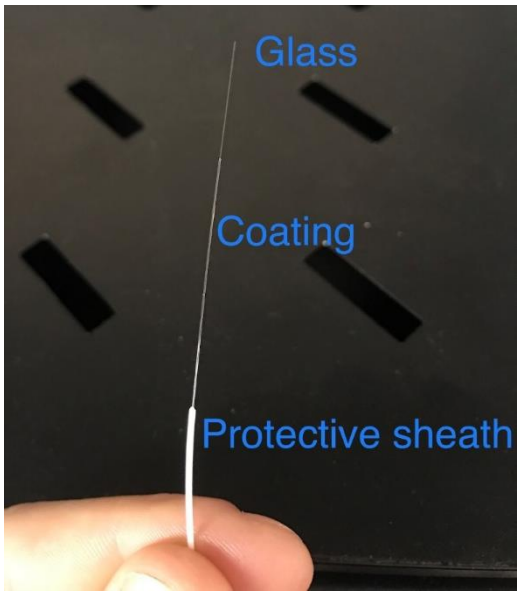

FIGURE 28: FIBRE'S STRUCTURE

The next step is to insert the two fibres into the machine at few millimetres and close the splicer, press the "SET" button and start the welding procedure. At the end of the welding, the machine conducts an optical verification to determine if the sequence went well or if there are losses in the transmission due to a wrong procedure. In this case, everything must be repeated. In figure 29 is shown the welding procedure.

FIGURE 29: WELDING PROCEDURE

4.7.3 Re-coater

After the welding, the fibre is still uncoated and needs to be protected with a polymeric material to reform the external coating. The fibre is inserted into a hermetical groove from which all the any solid residues or air bubbles are removed pressing the button “PURGE”. Then is possible to monitor the liquid polymeric material covering the fibre along its entire length from above. If the polymeric liquid does not cover the entire length of the uncovered fibre, it is possible to add material to complete the operation pressing the button “ADD”. In the end, the machine uses UV light to solidify the polymer around the fibre’s core. The machine is shown in figure 30.

FIGURE 30: RECOATER IN OPEN POSITION

4.7.4 Heat shrink tubing

The heat shrink protective sheath is a gum tube in which the fibre is inserted to provide further protection to the fibre from the external environment and to prevent excessive bending that can lead to the break of the fibre. The tube that has a bigger diameter, surrounds the fibre and then is heated to cover it tight and the result is as shown in figure 31.

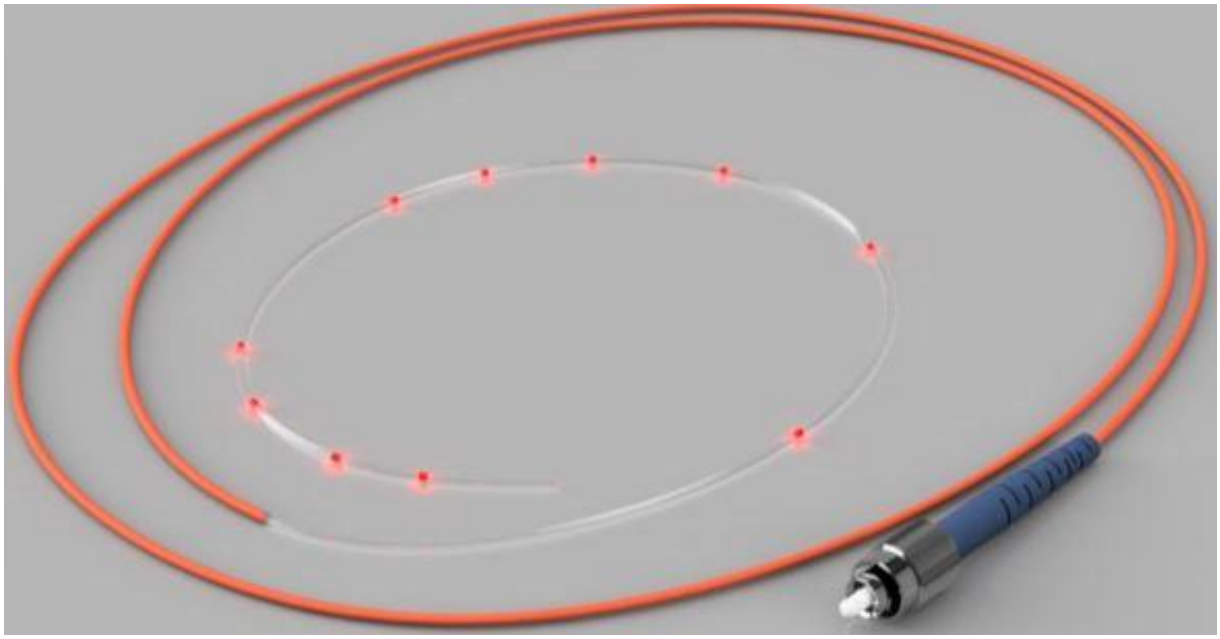

FIGURE 31: HEAT SHRINK TUBING

Chapter 5: Software description

In order to conduct the analysis of the tests executed are necessary a set of software to retrieve the information from the FBG sensor, from the Siemens accelerometer and to process the results. The software used in this thesis and their operation are described hereafter, in particular:

- SmartSoft V3.2: is the software used as interface between the computer and the interrogator [6].
- Siemens SINAMICS V-ASSISTANT software: is the tool to set the parameters of the V90 frequency converter.
- SM 1281 CMS software: This is the Condition Monitoring System software used to analyse the vibration pattern of the machine recorded by the accelerometer.
- Matlab scripts: all the scripts used to process the data collected during the tests.

5.1 SmartSoft V3.2

This software is the graphical interface for the SmartScan interrogator to be installed on a personal computer. It enables the operator to monitor and save the tests results obtained with the interrogator.

5.1.1 Connection with the computer

The connection between the interrogator and the computer is provided by a LAN cable, once the interrogator is turned on and correctly connected to the fibre is possible to launch the software and set it up. The first step required is to enter the IP address in the user interface as shown in figure 32:

FIGURE 32: IP ADDRESS SETTING WINDOW

The next step is to set the TCP/IPv4 settings in the computer following the procedure valid for Windows 10:

- Settings;
- Rete e internet;
- Ethernet;
- Modifica opzioni scheda;
- Ethernet;
- Protocollo Internet versione 4 (TCP/IPv4);
- Set the IP address as 10.0.0.1;
- Verify that the software is excluded from the firewall settings.

5.1.2 Setting up SmartSoft

In this work only one fibre with one Bragg sensor are used for the tests but, is possible to use up to 4 channels in which is possible to adopt several Bragg sensors in series in each channel. This can be useful if is required to retrieve several measurements along the same fibre in different position.
From the user interface is possible to set the data processing rate up to 25 kHz and is displayed a graph which shows the Bragg wavelength with the maximum peak value, as shown in figure 33.

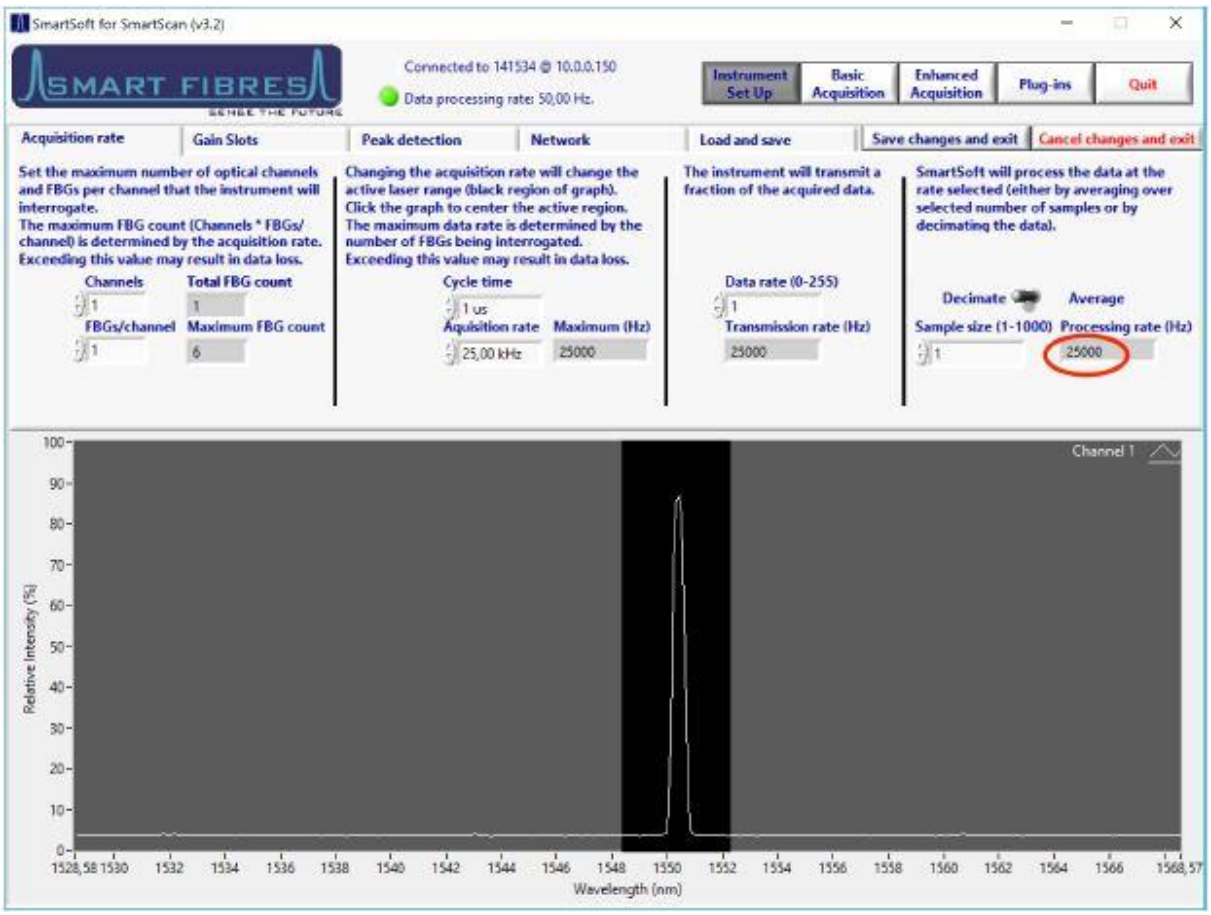

FIGURE 33: SMARTSOFT USER INTERFACE

If the sampling rate is increased, the active laser range will be reduced, and the inactive range is shown in grey.
In order to observe the vibration phenomenon of the PLA support, is necessary to choose properly the sampling rate. According to the Nyquist rule, is necessary to sample data with a frequency at least 10 times higher than that of the phenomenon observed so, we used the higher frequency possible that is 25 kHz.
At this high frequency is necessary to limit the duration of the test to about 1/2 seconds to avoid excessive amount of data. In this way, the acquisition file is not too big to be processed by the Matlab scripts.

As already mentioned, the Bragg sensor reflects a certain wavelength from the laser beam generated by the interrogator. This information can be processed to obtain the desired measurement such as temperature, strain and pressure.
From the "Enhanced Acquisition" window is possible to obtain the data pressing the button "Log" but only after a destination for the *.log* file is selected. After the acquisition, the *.log* file is available to be processed by the Matlab scripts.
A problem to be overcome is that data are usually saved before the pressing of the "Log" button, probably because there is a delay caused by buffer overflow.
Another function available in this software is to display a Fourier spectrum in real time through the window "plug-ins" selecting "FFT plug-in", in this way the raw data are shown directly on video and in real time as shown in the example of figure 34 [6].

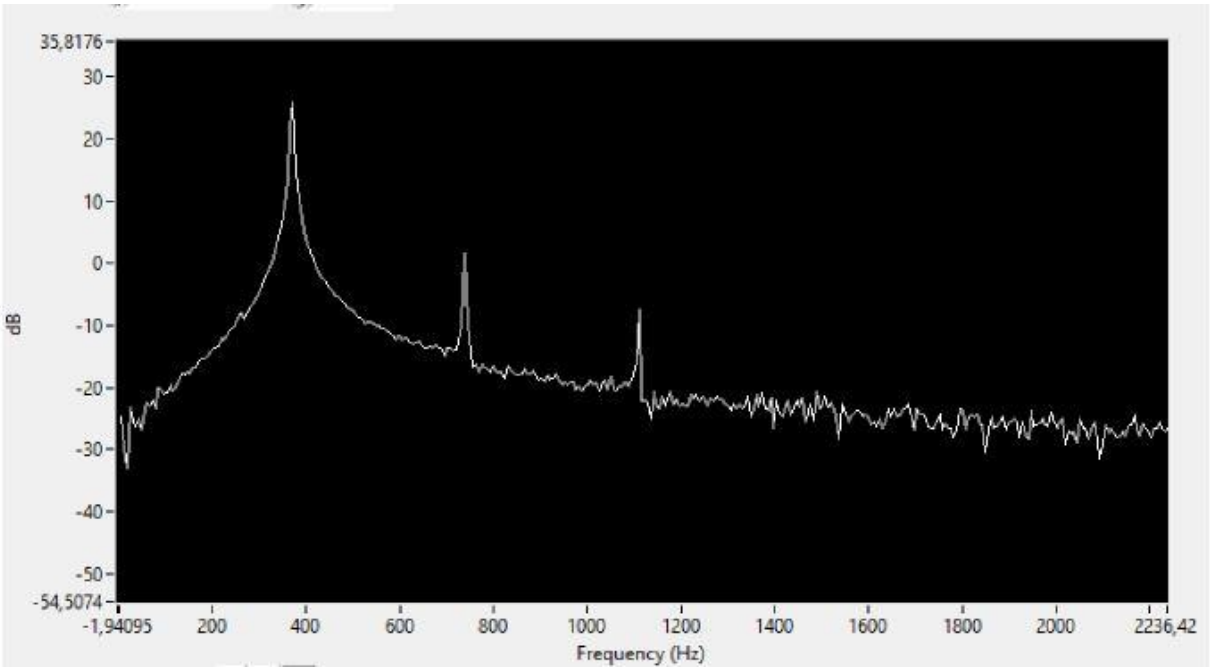

FIGURE 34: FFT PLUG-IN EXAMPLE

5.2 Siemens SINAMICS V-ASSISTANT

The SINAMICS V-ASSISTANT engineering tool has been designed to speed up commissioning in service and diagnostics of SINAMICS V90 frequency converters with interface PROFINET. The software works on a personal computer with Windows operating systems, use the graphical interface to interact with users and communicates with the SINAMICS V90 PN frequency converter via USB. It can be used to change the parameters and monitor the status of the SINAMICS V90 drive [7].

5.2.1 parametrization

Since all the electronics are already supplied and ready to use, in this chapter are shown the available functions for the v90 parameters control.
As shown in figure 35, in the left menu of the SINAMICS V ASSISTANT there are four available functions to control the parameters, which are:

- Ramp function configuration;
- Limits settings;
- Input/output configuration;
- Display of all parameters.

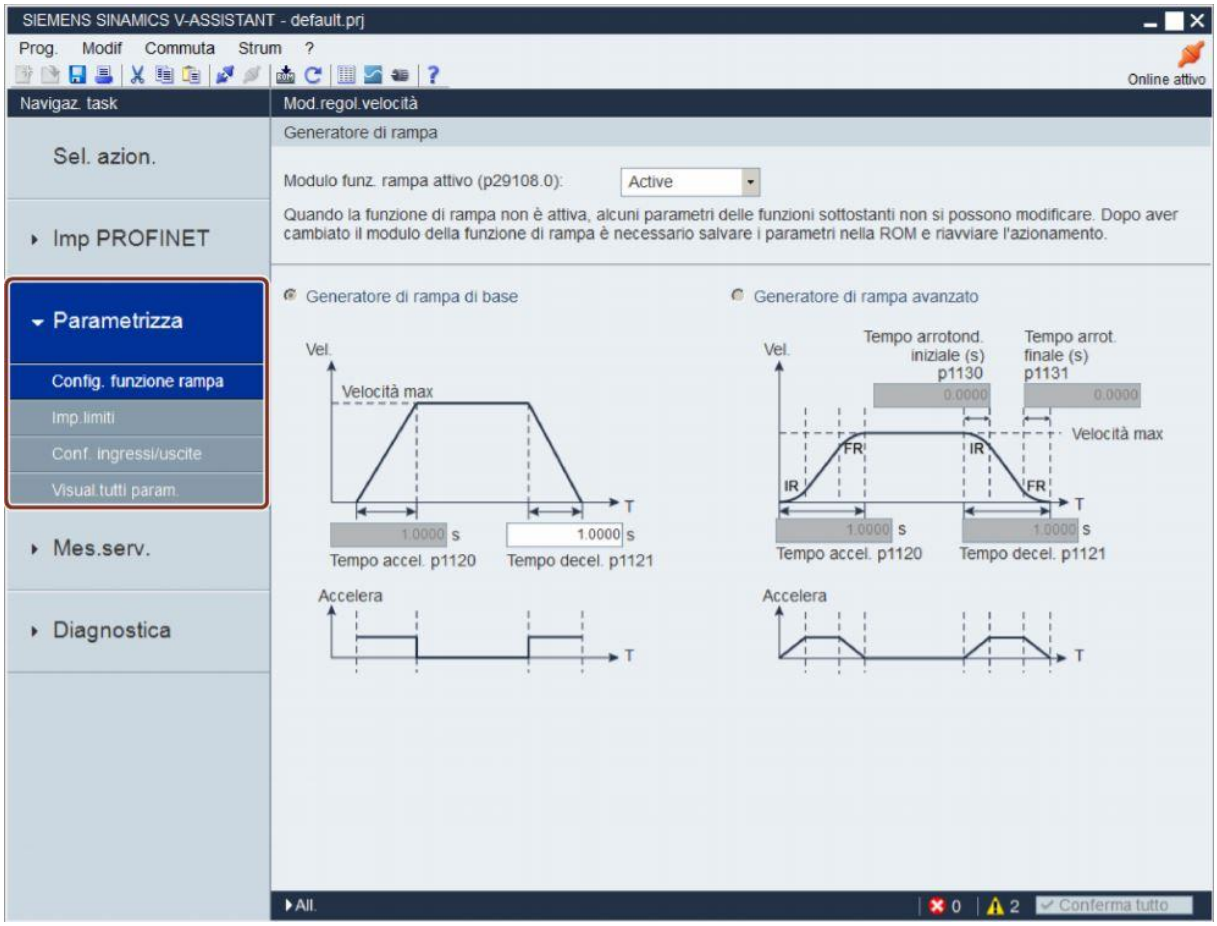

FIGURE 35: SINAMICS V ASSISTANT USER INTERFACE

Ramp function configuration:

The ramp generator is used to limit acceleration in the event of abrupt changes of the reference value and thus helps to prevent overloads during the drive operation.
The ramp time p1120 and the deceleration time p1121 can be used for setting the acceleration and deceleration ramps separately. This allows for a smooth transition in case of changes of the reference value.
There are two types of basic ramp generator. Parameters can be specified in the corresponding panels:

- Basic ramp generator

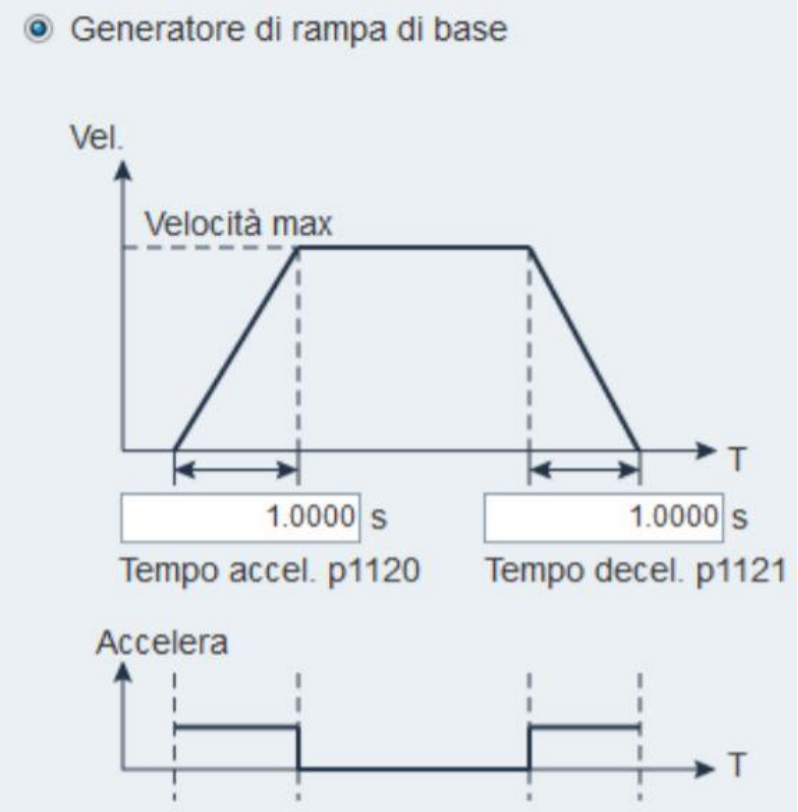

FIGURE 36: BASIC RAMP GENERATOR

- Advanced ramp generator

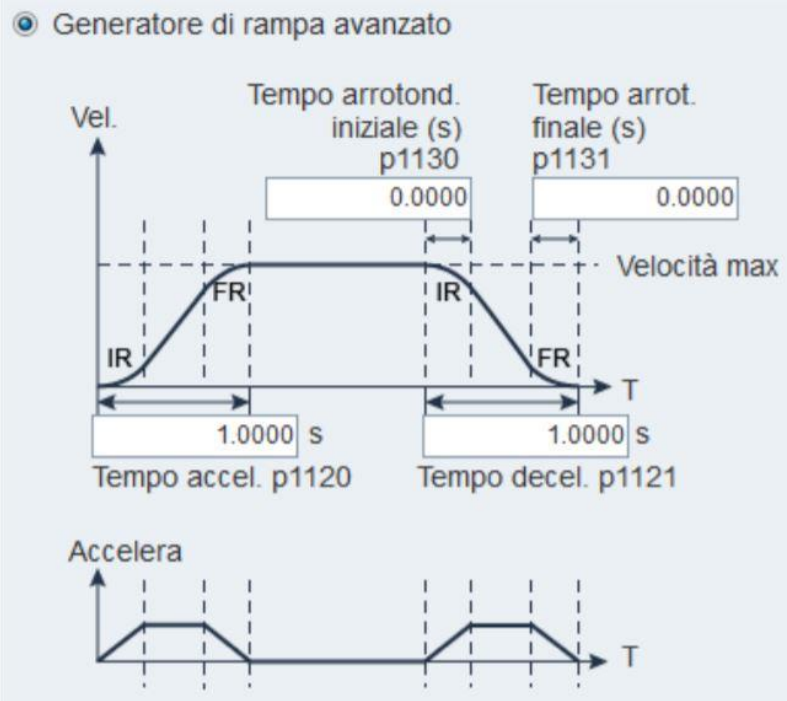

FIGURE 37: ADVANCED RAMP GENERATOR

Limits settings:

- Torque limit can be specified in the following panel

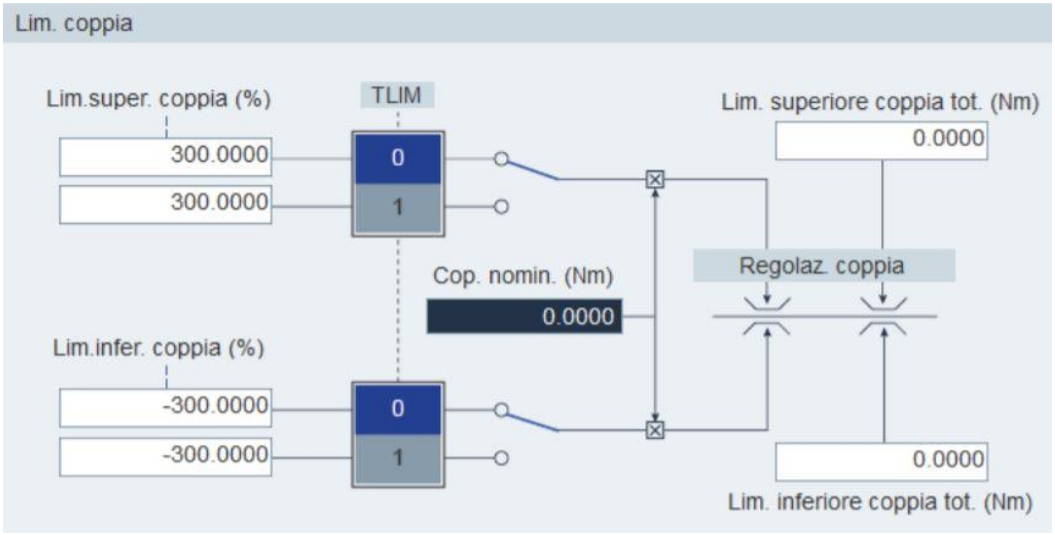

FIGURE 38: TORQUE LIMIT SETTING

- Velocity limit can be specified in the following panel

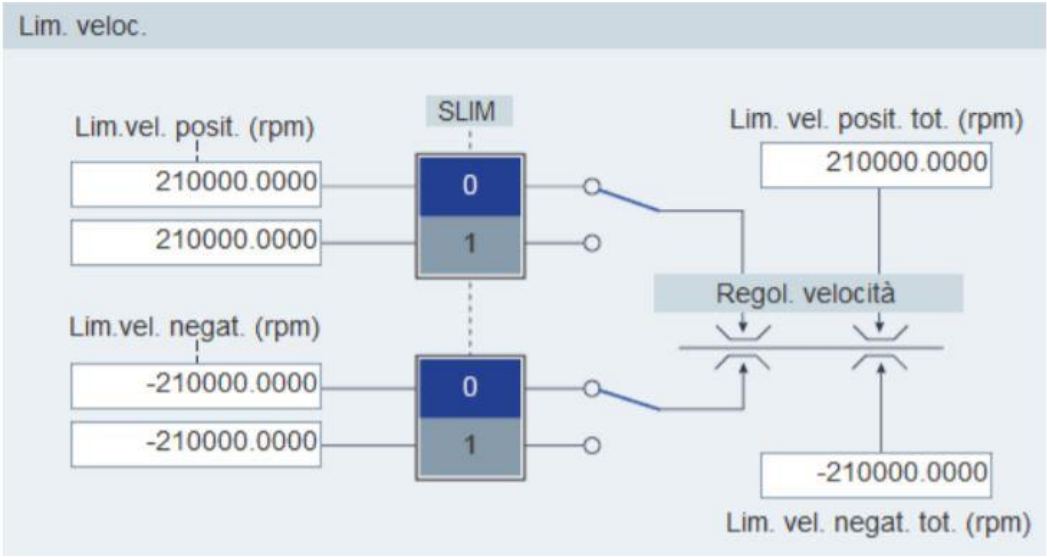

FIGURE 39: VELOCITY LIMIT SETTING

Input/output configuration:

Digital inputs can be assigned in the following panel:

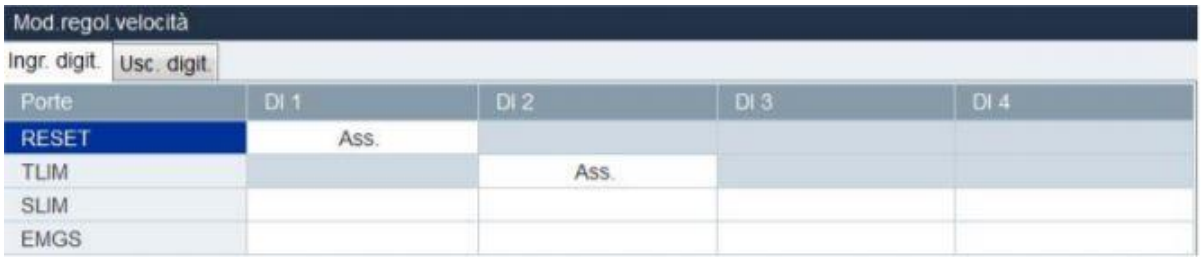

FIGURE 40: DIGITAL INPUTS PANEL

In total four signals can be freely connected to digital inputs; Click on the cells with a white background in the table. In the list box two options appear: Assign and Cancel. Select "Assign" to connect the input digital to the corresponding signal. The current row turns gray. Otherwise select "Cancel" to remove the link. The current row is displayed in white.

Digital outputs can be assigned in the following panel:

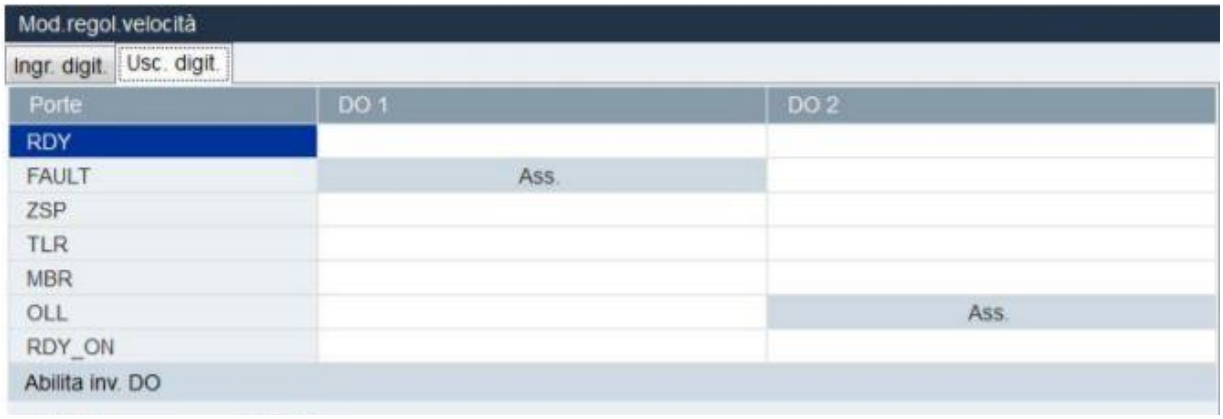

FIGURE 41: DIGITAL OUTPUTS PANEL

In total, seven signals can be freely connected to digital outputs. Click on the cells with a white background in the table. Select "Assign" to connect digital input to the corresponding signal. The current cell turns gray.

Display of all parameters:

All modifiable parameters can be configured in this field:

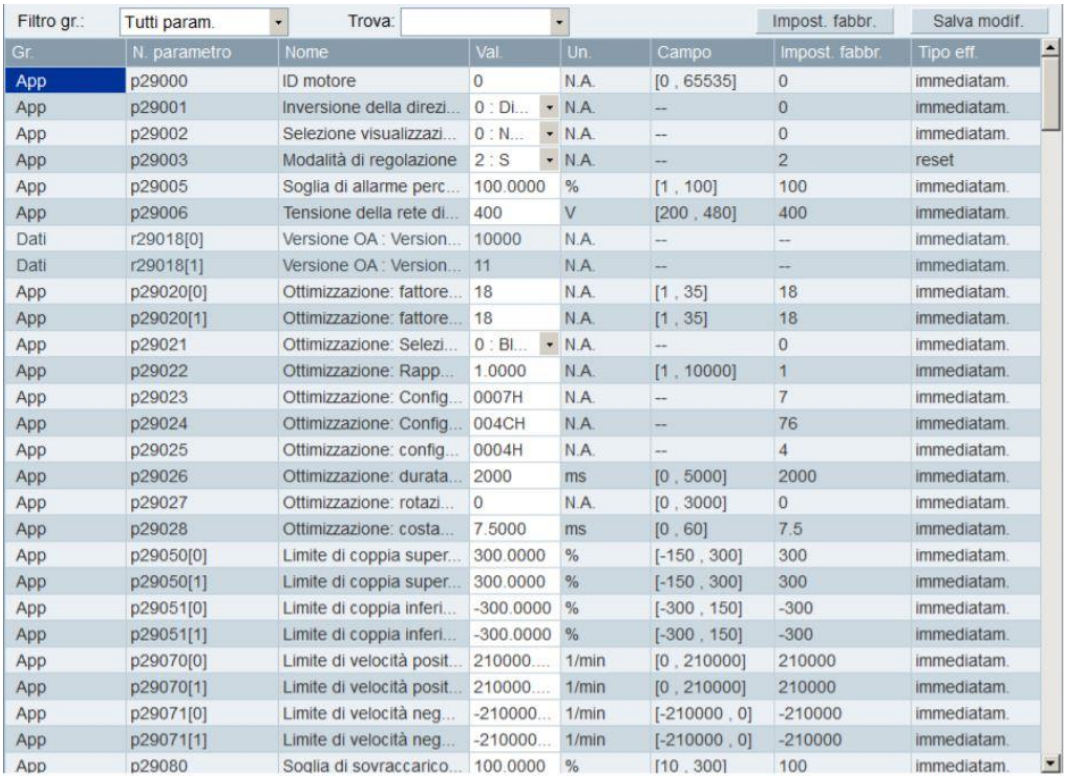

Filtro gr.: Tutti param. Trova: Impost. fabbr. Salva modif.

Gr.	N. parametro	Nome	Val.	Un.	Campo	Impost. fabbr.	Tipo eff.
App	p29000	ID motore	0	N.A.	[0 , 65535]	0	immediatam.
App	p29001	Inversione della direzi...	0 : Di...	N.A.	--	0	immediatam.
App	p29002	Selezione visualizzazi...	0 : N...	N.A.	--	0	immediatam.
App	p29003	Modalità di regolazione	2 : S	N.A.	--	2	reset
App	p29005	Soglia di allarme perc...	100.0000	%	[1 , 100]	100	immediatam.
App	p29006	Tensione della rete di...	400	V	[200 , 480]	400	immediatam.
Dati	r29018[0]	Versione OA : Version...	10000	N.A.	--	--	immediatam.
Dati	r29018[1]	Versione OA : Version...	11	N.A.	--	--	immediatam.
App	p29020[0]	Ottimizzazione: fattore...	18	N.A.	[1 , 35]	18	immediatam.
App	p29020[1]	Ottimizzazione: fattore...	18	N.A.	[1 , 35]	18	immediatam.
App	p29021	Ottimizzazione: Selezi...	0 : Bl...	N.A.	--	0	immediatam.
App	p29022	Ottimizzazione: Rapp...	1.0000	N.A.	[1 , 10000]	1	immediatam.
App	p29023	Ottimizzazione: Config...	0007H	N.A.	--	7	immediatam.
App	p29024	Ottimizzazione: Config...	004CH	N.A.	--	76	immediatam.
App	p29025	Ottimizzazione: config...	0004H	N.A.	--	4	immediatam.
App	p29026	Ottimizzazione: durata...	2000	ms	[0 , 5000]	2000	immediatam.
App	p29027	Ottimizzazione: rotazi...	0	N.A.	[0 , 3000]	0	immediatam.
App	p29028	Ottimizzazione: costa...	7.5000	ms	[0 , 60]	7.5	immediatam.
App	p29050[0]	Limite di coppia super...	300.0000	%	[-150 , 300]	300	immediatam.
App	p29050[1]	Limite di coppia super...	300.0000	%	[-150 , 300]	300	immediatam.
App	p29051[0]	Limite di coppia inferi...	-300.0000	%	[-300 , 150]	-300	immediatam.
App	p29051[1]	Limite di coppia inferi...	-300.0000	%	[-300 , 150]	-300	immediatam.
App	p29070[0]	Limite di velocità posit...	210000....	1/min	[0 , 210000]	210000	immediatam.
App	p29070[1]	Limite di velocità posit...	210000....	1/min	[0 , 210000]	210000	immediatam.
App	p29071[0]	Limite di velocità neg...	-210000...	1/min	[-210000 , 0]	-210000	immediatam.
App	p29071[1]	Limite di velocità neg...	-210000...	1/min	[-210000 , 0]	-210000	immediatam.
App	p29080	Soglia di sovraccarico...	100.0000	%	[10 , 300]	100	immediatam.

FIGURE 42: DISPLAY OF ALL PARAMETERS

All the parameters are displayed with the following information:

- Group;
- Parameter number;
- Name;
- Value;
- Unit;
- Field;
- Factory setting;
- Type of effect.

Note that all the values displayed white cells are modifiable.

5.3 SM 1281 CMS software

This is the software coupled with the Condition Monitoring System used to analyse more precisely the vibration pattern of the machine recorded by the accelerometer.
Using the SM 1281 is possible to monitor the states of components subject to wear, e.g. motors, bearings, and critical machine components. Indeed, most types of damage are recognizable in the spectrum by the occurrence of typical damage frequencies [8].
The software can calculate the vibration acceleration spectrum as a basis for vibration diagnosis and monitoring. The principle of frequency analysis is to convert a signal from the time band into the frequency band by means of spectral analysis. One common mathematical method is the Fast Fourier Transform.
There are two main modes to be used for our purposes:

- Measurement mode is for test purposes and to support commissioning to define the limits to be monitored. In measurement mode, measured variables chosen by the user are measured, calculated and displayed as spectra. Spectra can be saved as fingerprints and record of the current machine condition regarding vibration.
- In monitoring mode, all measured variables to be monitored are constantly measured, calculated and monitored for parameterized limits. If limit values are exceeded, relevant messages are output, and the parameterized responses are executed.

5.3.1 Monitoring of machine vibration variables

Before starting to perform a measurement on the machine is necessary to have a reference condition of the machine in the fault-free condition as a frequency spectrum.
The first step is to assign limit bands on the measurements, the violation of which indicates the fault of the machine condition.
On the “Monitoring settings” (1) is possible to set the limit values as limit bands (2) and also warning and alarm limits (3).
In the next figure is shown the basic speed-related monitoring (4).

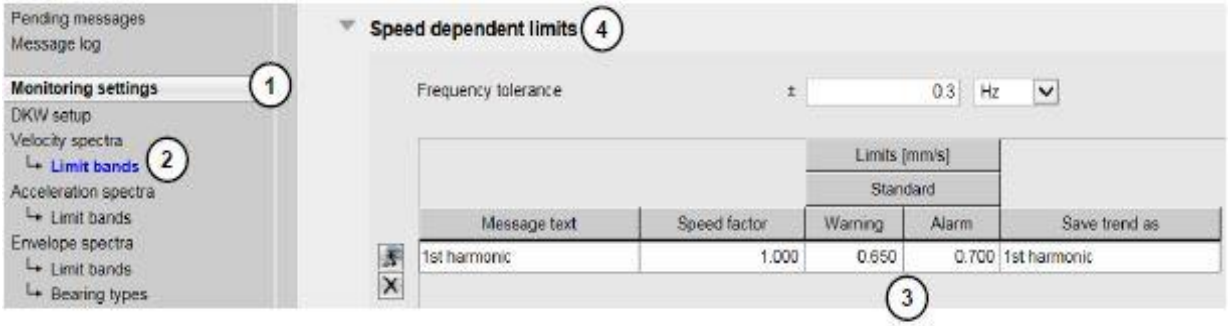

FIGURE 43: SPEED DEPENDENT MONITORING

Hereafter is explained how to perform such measurement via the HMI/user program:

1. Activate the “S7 priority” on the HMI

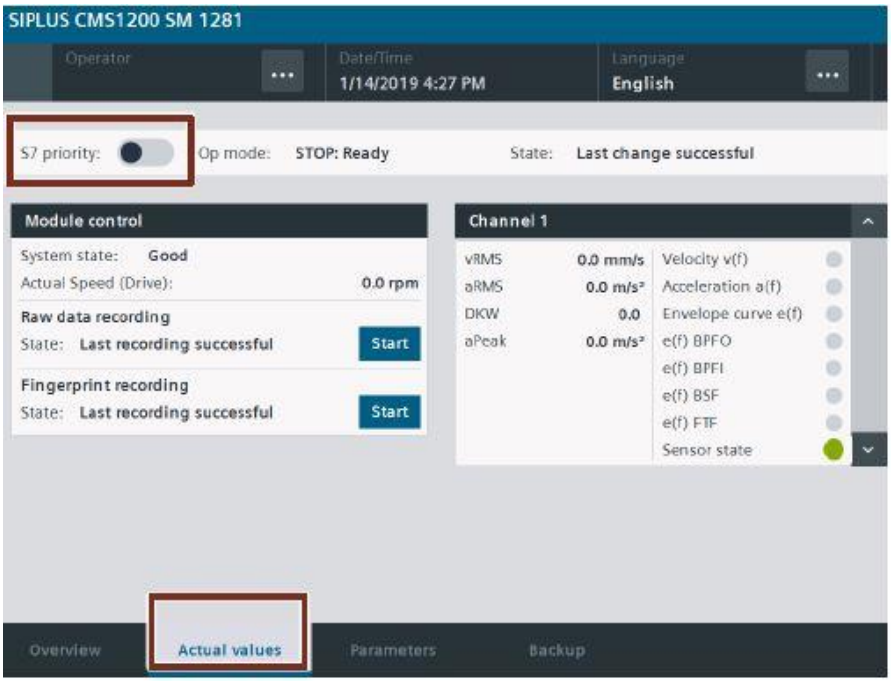

FIGURE 44: HMI INTERFACE

2. Switch the operating mode to “RUN: Monitor”;

3. Start the machine on the HMI: Tab “Overview” → Input setpoint speed → “Enable drive”;

4. Tap on “Start” to start the fingerprint recording, the frequency spectrum is saved under a name assigned by the system.

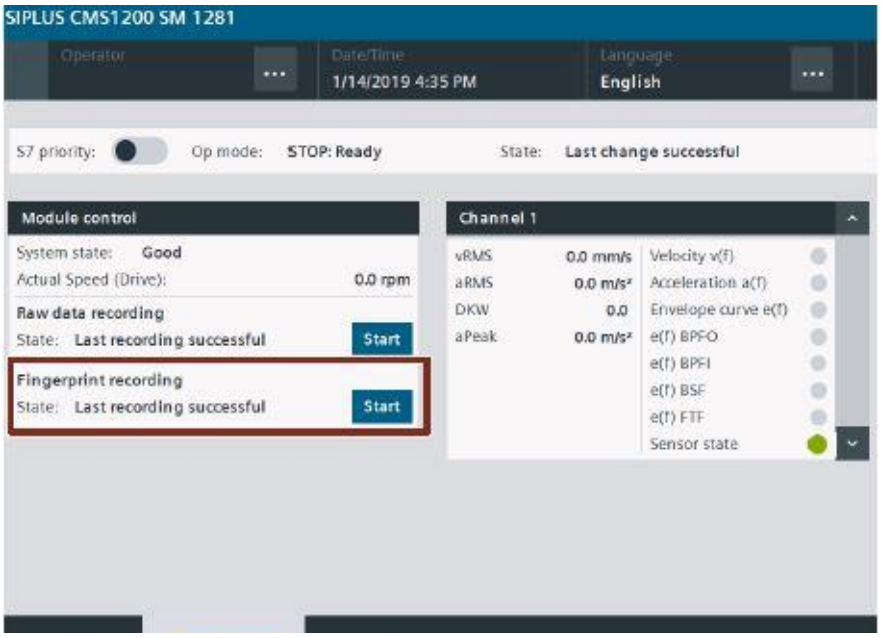

FIGURE 45: HMI INTERFACE

The frequency spectrum obtained by the measurement is as the example in figure 46, in which are displayed the warning and alarm limits including the parameterized frequency tolerance.

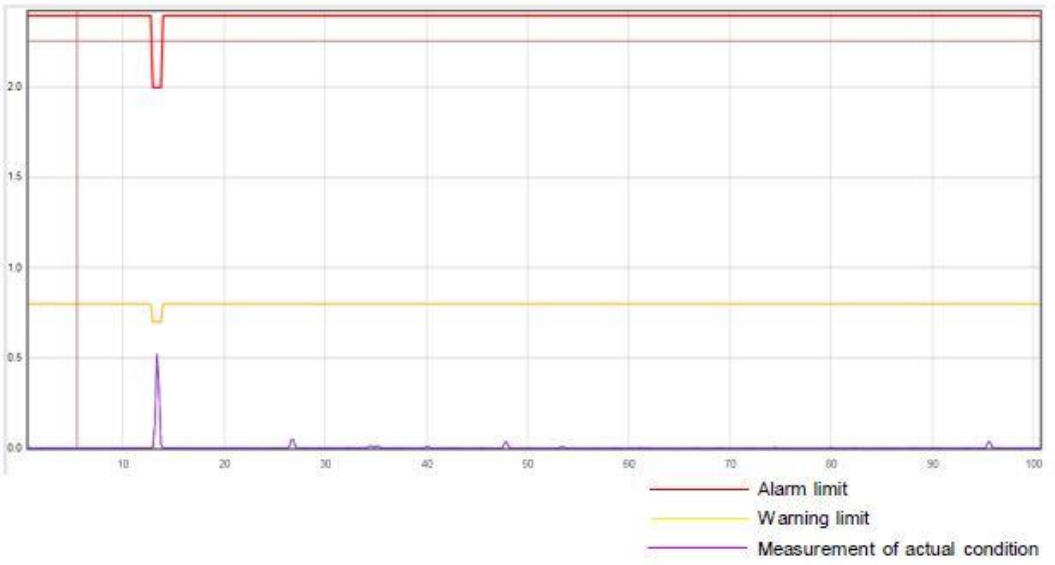

FIGURE 46: FREQUENCY SPECTRUM

The typical characteristic expected to appear in the event of unbalance of the machine, as our case, is like the graph in figure 47:

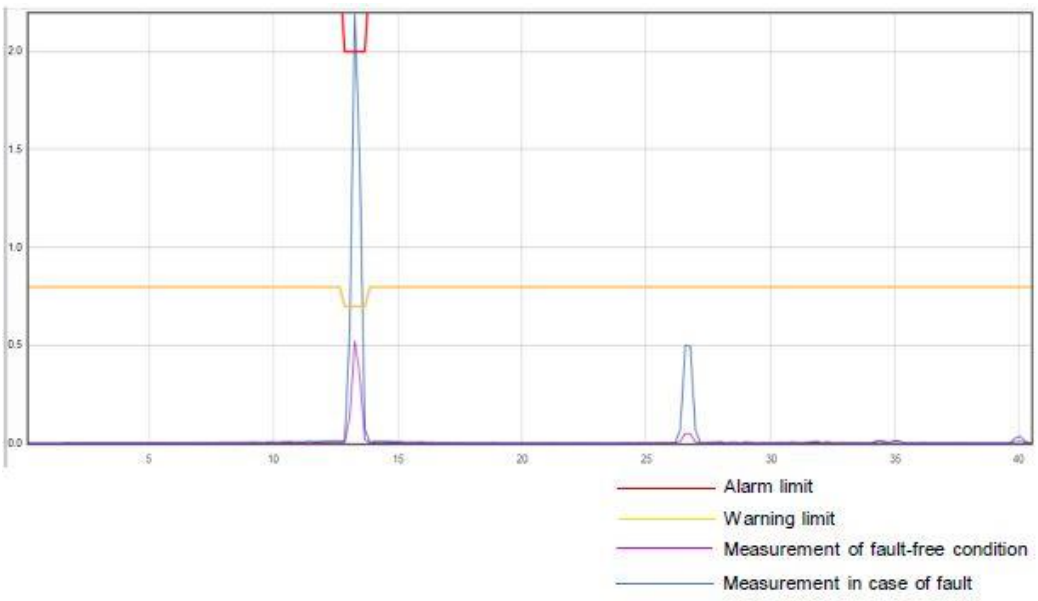

FIGURE 47: FREQUENCY SPECTRUM IN CASE OF UNBALANCE

Is possible to notice the formation of damage frequencies which violate the alarm and warning limit, this verifies signs of wear on the machine. So, in case of damage to the machine the graph shows the following characteristics:

- The amplitude of the damage frequencies falls as the frequency increases;
- In the graph appear harmonics: the frequency associated to the damage are integer multiples of the machine rotational speed.

5.4 Matlab script for FBG sensor

As anticipated, all the data acquired from the SmartSoft software are saved into *.log* files that can be read and processed by the Matlab script. The purpose of the code is to use the Fourier analysis and to show the oscillation frequency indicated by the FBG sensor.
The Fourier analysis is useful because it can interpret any signal and reconstruct it through an infinite sum of sinusoidal contributions. For this reason, we expect a predominant sinusoid from the analysis that indicates the oscillation frequency recorded, since the motion is imposed by the electronic motor controlled by the parameters set in the V90 controller. So, the script starting from the raw data can plot the Fourier spectrum and show the predominant peak that indicates the sinusoid with the maximum amplitude. The peak shown is the indication of the measurement of the frequency oscillation of PLA support.
The main features of the Matlab script are [9]:

- Automated acquisition: the raw data generated by SmartSoft and saved into *.log* files are automatically extracted by a function called "IMPORTFIBRAFUNCTION.m".
- The Fourier spectrum is shown also in a logarithmic scale.
- Determines the peaks and the effective oscillation amplitude.

The script used in this thesis is shown below:

```
clear all; close all;
% - - - - - INPUT DA INTERROGATORE  - - - - %
% Legge il file convertito da .log
percorso = "C:\Users\ricca\Documents\MATLAB\Tesi
Matlab\vibrazionefibra.log";
freq_camp = 25000;                  % Frequenza di
campionamento
TZ = IMPORTFIBRAFUNCTION(percorso);
% ------------------------------------------------------
-----------------------------------------
% - - - - - Estrazione dei dati RAW - - - - %
t = TZ(:,1);                        % Micros
t_sec = t/1e6;                      % Trasformo i micros in
secondi
z = TZ(:,2);                        % Accelerazione acquisita
(1 solo asse)
zmax=max(z);zmin=min(z);
figure
subplot(3,2,[1 2])
plot(t_sec,z,'b','marker','o')    % Plotto le lunghezze
d'onda e il tempo in secondi
xlabel("Time [s]"); ylabel("\lambda [nm]"); title("RAW");
% - - - - - Analisi di Fourier - - - -%
L = length(z);                      % Lunghezza del segnale
```

```
Y = fft(z);                          % Calcola la trasformata
di Fourier del segnale
P2 = abs(Y/L);                       % Calcolo dello spettro
(2 lati) P2
P1 = P2(1 : L/2 +1);                 % Calcolo dello spettro
singolo
P1(2:end-1) = 2*P1(2:end-1);         % Calcolo di "even valued
signal length L"
f = freq_camp * (0:(L/2))/L;         % Definizione del dominio
della frequenza
% - - Individuazione del primo picco - -  %
[picco, indicepicco] = max( P1(10:end) );
% Escludo i primi 9, perche' e' sempre presente un massimo
a frequenza = 0
freq = f(indicepicco + 9)            % Riparto dall'indice 9
picco
AMPIEZZA = zmax-zmin;                % Calcolo (approssimato)
dell'ampiezza
resolution= f(2)-f(1);                % Risoluzione dello
spettro di Fourier
% - - - - - Individuazione di altri picchi - - - - %
tol = picco/5; j=1;                  % Tolleranza
for i=indicepicco+10:length(f)
    if P1(i)>tol
        freq2 = f(i)
        secondopicco(j) = P1(i)
        j=j+1;
    end
    i=i+1;
end
% - - - - - - Grafici - - - - - - %
subplot(3,2,[3 4])
plot(f,P1)
xlabel("Frequency [Hz]"); ylabel("Amplitude (linear)
[nm]");
title("FOURIER ANALYSIS: Single-Sided Amplitude
Spectrum");
axis([1, 3000, -1, picco+1]);
subplot(3,2,[5 6])
semilogy(f,P1,'r')
xlabel("Frequency [Hz]"); ylabel("Amplitude (logaritmic)
[nm]");
title("FOURIER ANALYSIS: Single-Sided Amplitude
Spectrum");
axis([1, 3000, -1, picco+1]);
```

Moreover, the graphs displayed at the end of the processing are as the example in figure 48:

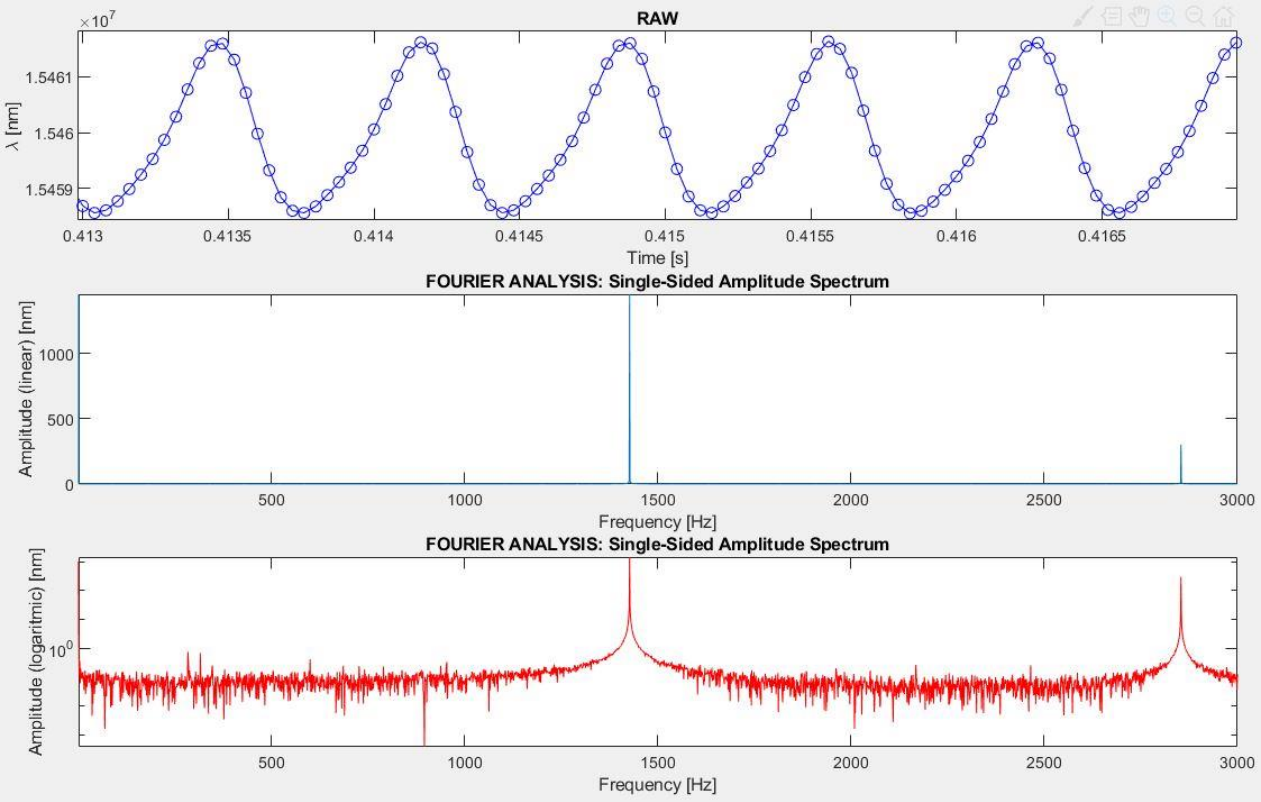

FIGURE 48: MATLAB PLOT EXAMPLE

Chapter 6: Tests

All the tests and the observations are reported in this chapter in detail. The behaviour of the fibre and how it is influenced by certain factors such as pretension will be shown. The first step was to calculate fibre's resonance frequency and to compare it with a theoretical estimate, after that, the fibre has been glued to the 3D printed PLA support. Finally, some tests carried out with the mechanical shaker are shown in detail. For a complete study of the support, is also shown a dynamic simulation for the support when it is mounted on the mechanical shaker.

6.1 Vibrating String theory

In previous thesis works carried out at Politecnico di Torino has been demonstrated that the fibre behaves like a vibrating string. Indeed, it was noticed that at certain frequency of forced sinusoidal motion the oscillation of the fibre increases. It must be considered that every system, when subjected to a sinewave command with a frequency near its natural frequency, starts to amplify the input value. Obviously, this phenomenon must be avoided as it can lead to breakage of the fibre. So, it is important to know the fibre's natural frequency in order to understand if the phenomenon observed and monitored can lead to resonance. Its own natural frequency can be calculated using the vibrating string theory which tells us [2]:

$$f = \frac{1}{2L}\sqrt{\frac{T}{\rho}}$$

Where:

- L is the suspended fibre length;
- T is the tension to which the fibre is subjected, measured in [N];
- ρ is the linear density of the fibre, in [kg/m].

The fibre's tension T can be easily computed using the following formulation given by the Hooke's law:

$$T = E \cdot A \cdot \frac{\Delta L}{L} = E \cdot A \cdot \varepsilon$$

Where:

- E is the Young modulus of the fibre;
- A is the section's area of the fibre;
- ε is the strain to which the fibre is subjected.

Since the area A and the Young modulus E are known, changing the ε value through the micro-positioner is possible to obtain the desired T value and consequently the natural frequency of the fibre. In previous thesis works the mean Young modulus and the linear density of the fibre has been already found and they are listed in the table below [9]:

TABLE 4: OPTICA FIBRE'S DATA

Optical fibre's data	
Fibre length [m]	0.1
Section's area A [m^2]	$4.9 \cdot 10^{-8}$
$\rho_{coating}$ [kg/m^3]	1160
ρ_{glass} [kg/m^3]	2650
Mean ρ [kg/m]	$7.523 \cdot 10^{-5}$
Young modulus E [GPa]	17

Where the mean linear density was obtained with:

$$\rho = (\frac{3}{4}\rho_{coating} + \frac{1}{4}\rho_{glass}) \cdot A$$

Considering that the S-1FL6 brushless motor nominal speed is about 3000 rpm, the related vibration generated by the eccentric mass will never exceed 50 Hz during the tests. So, it is necessary that the resonance frequency of the fibre is higher enough than the value of rotation speed with some margin. In this way, it is enough to tense the fibre over a certain value.
Now will be shown the calculations to obtain a resonance frequency that is one or two orders of magnitude greater than that of the test bench rotation.

6.2 Fibre pre-tensioning

Assuming we wanted to get a natural frequency above 50 Hz, with the previous information already know, we need to find the strain value ε beyond which this is verified. The previous formula for the vibrating string theory was implemented in Matlab to show how the frequency varies with the μstrain, as can be seen in figure 49.

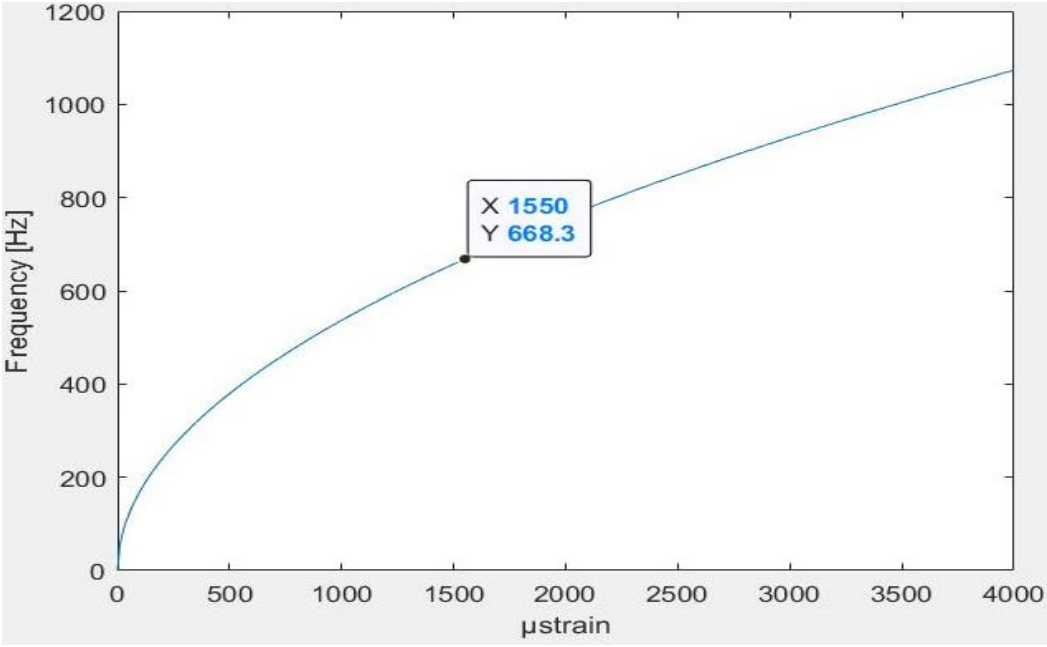

FIGURE 49: μSTRAIN VS FREQUENCY

Considering that the fibre will drop the tension after the gluing and cap installation, the fibre has been pretensioned to a value of approximately 1500 μstrain to be conservative. This let us expect to reach a resonance frequency around 600 Hz to decrease. In the end the fibre has been glued with cyan acrylic glue to the support following this procedure:

- Positioning of the FBG sensor in the centre of the support;
- Gluing the fibre to the support in the side of which the interrogator is connected;
- Gluing the opposite free end of the fibre to the micro handler;
- Tensing the fibre with the micro handler monitoring through SmartSoft the strain, until reaching the desired value of about 1500 µstrain as shown in figure 50;
- Gluing the fibre to the support and wait 24 hours to dry as shown in figure 51;
- Cover the top of the support with the cap glued as well to double the gluing surface;
- Wait for the glue to dry long enough and then cut the fibre to the side connected to the micro handler.

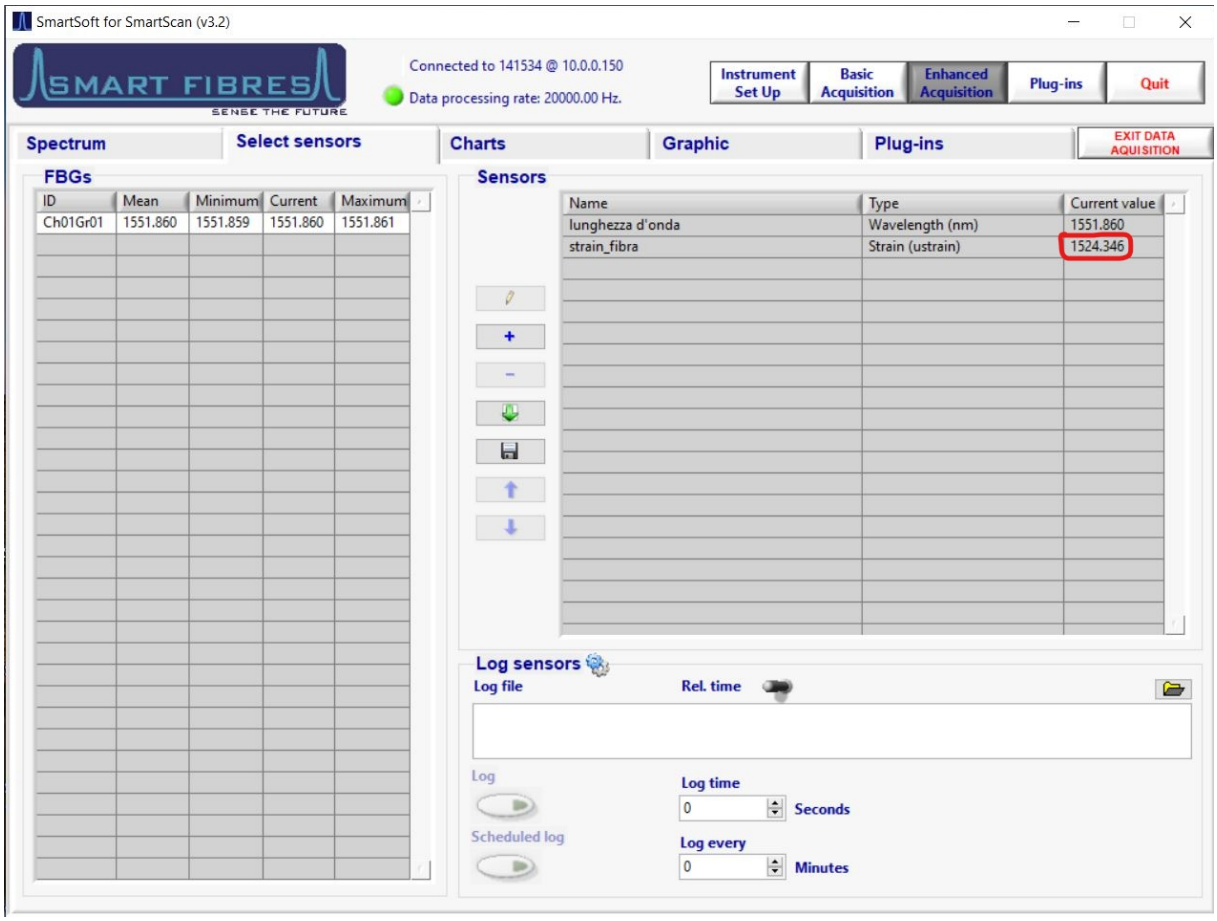

FIGURE 50: STRAIN MEASUREMENT

It's important to remember that it is not necessary to obtain a precise strain value for the fibre since the aim is to obtain a resonance frequency high enough to be avoided during the tests. So, taking into account that and the tension drop after installation, has been decided to tense the fibre at 1500 μstrain to be conservative. Finally, the FBG sensor for vibration monitoring of the bearing support is ready to work and is shown in figure 52.

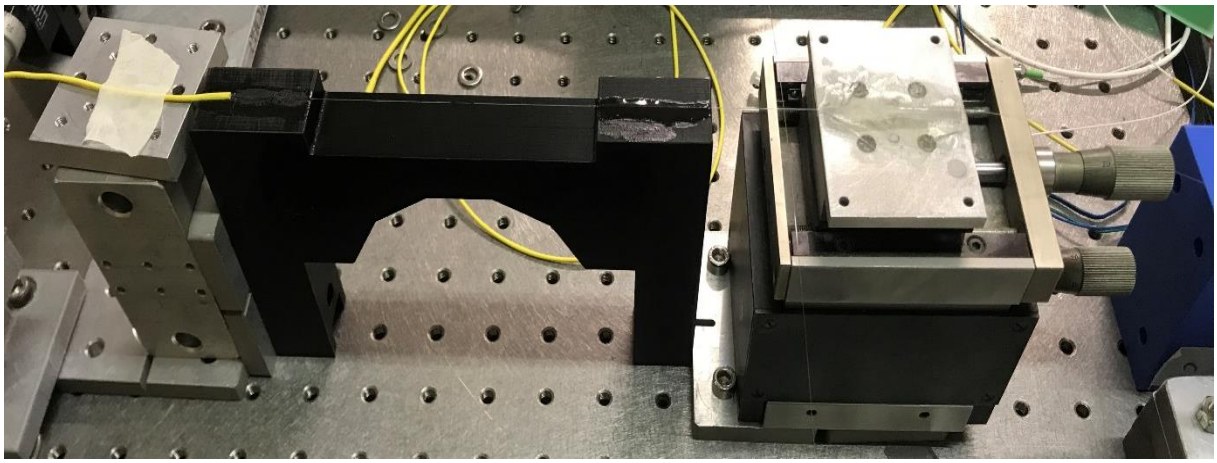

FIGURE 511: GLUING THE FIBRE

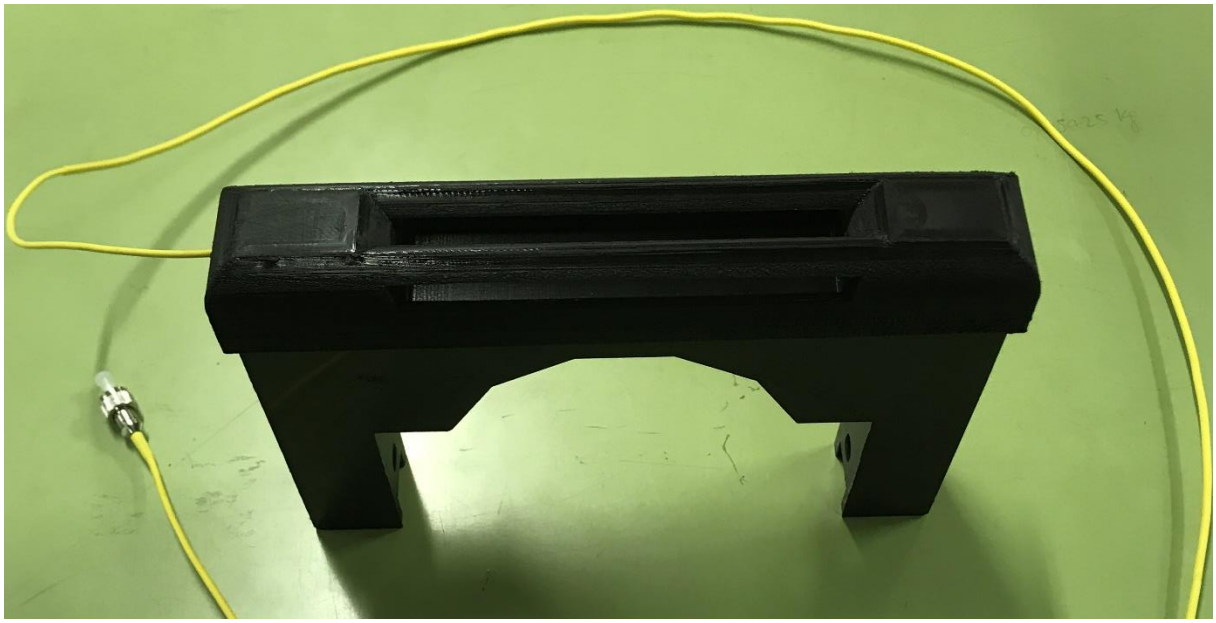

FIGURE 52: FBG 3D PRINTED SUPPORT COMPLETED

6.3 Mechanical shaker tests

In order to conduct some tests and verify that the resonance frequency of the fibre is high enough to avoid the phenomenon during the operation on the vibration test bench, the FBG support has been temporary modified to be adapted to the mechanical shaker. As shown in figure 53, it has been glued a screw on the bottom side of the support to permit the physical connection to the shaker.

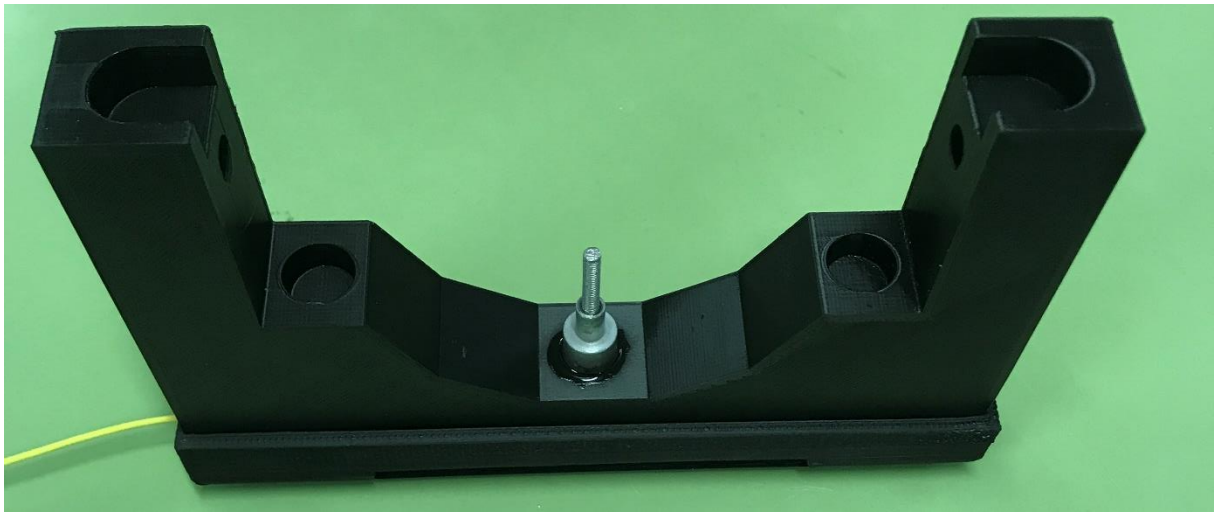

FIGURE 52: THE FBG SUPPORT MODIFIED

Once the glue dried, two tests has been carried out with the mechanical shaker, one generic test to verify the functionality of the sensor and the other to find out the resonance frequency of the fibre. In figure 54 is shown the FBG sensor support connected with the mechanical shaker.

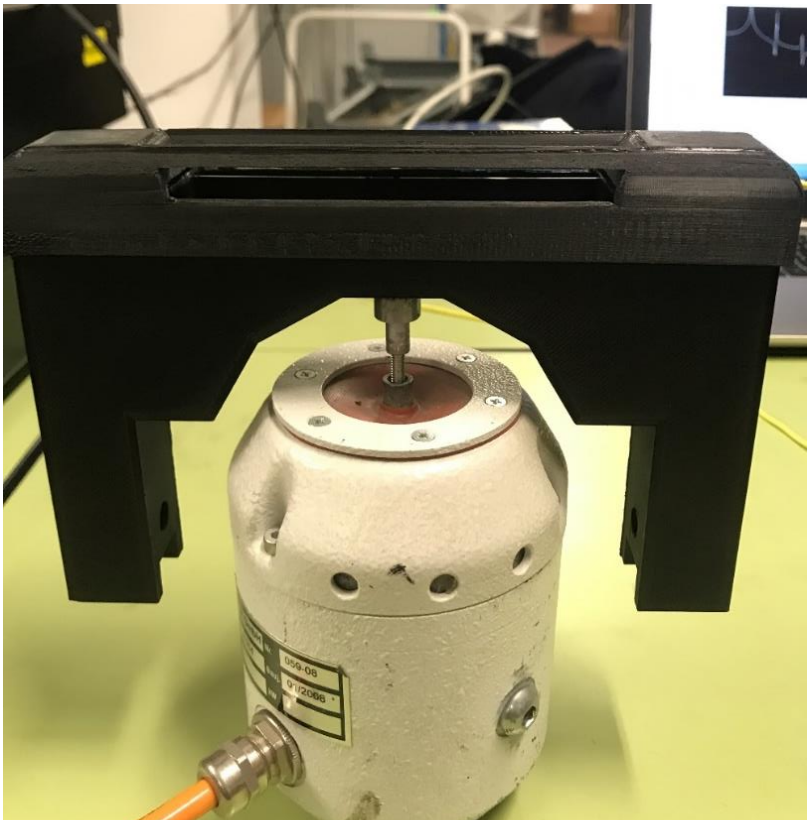

FIGURE 53: FBG SUPPORT MOUNTED ON THE SHAKER

6.3.1 Generic frequency test

The first test has been carried out by setting a frequency of 300 Hz on the function generator and a log time of 1 second on the SmartSoft software. The generated file has been processed by the Matlab script that has produced the following graphs in figure 55.

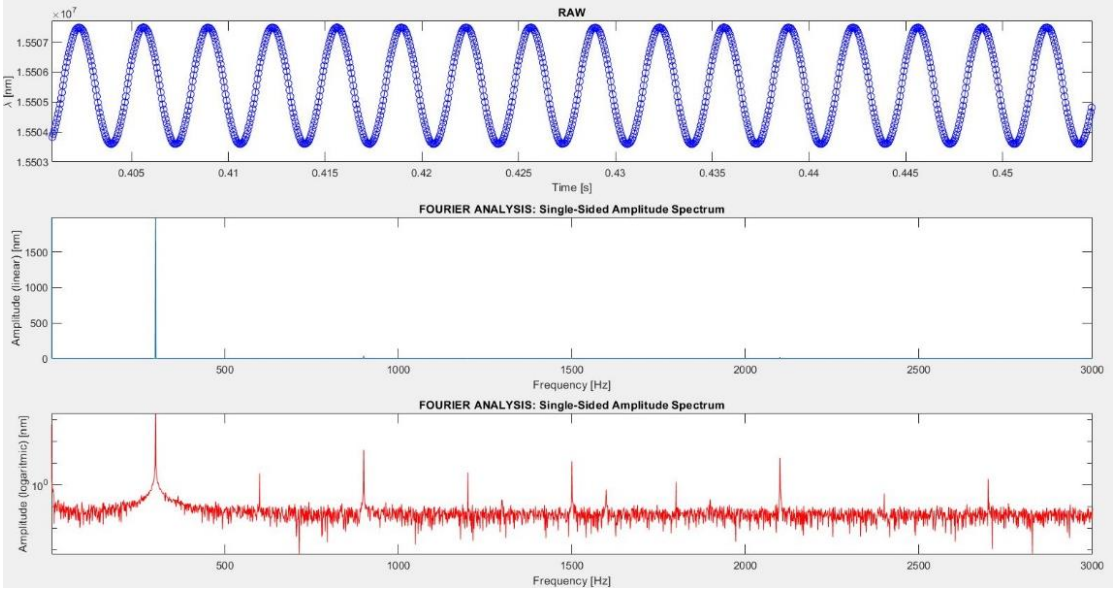

FIGURE 54: MATLAB PLOT FOR THE VIBRATION TEST

During the test, the fibre was clearly stationary as the resonance frequency has not been reached and the Fourier analysis plotted by the script shows that the FBG sensor senses the exact frequency imposed by the function generator. Although the fibre seems stationary, the Bragg grating returns the exact frequency of excitation. This can be explained by the fact that PLA support deforms during the motion. Indeed, the FBG detects the stretching of the fibre associated with a wavelength increase and the compression of the same highlighted by a decrease in the wavelength. Via Solidworks, has been carried out a simulation test to find out the vibration modes of the support in the constraint condition of the mechanical shaker, as we expected, the mode of vibration in the direction of the excitation acts like shown in figure 56.

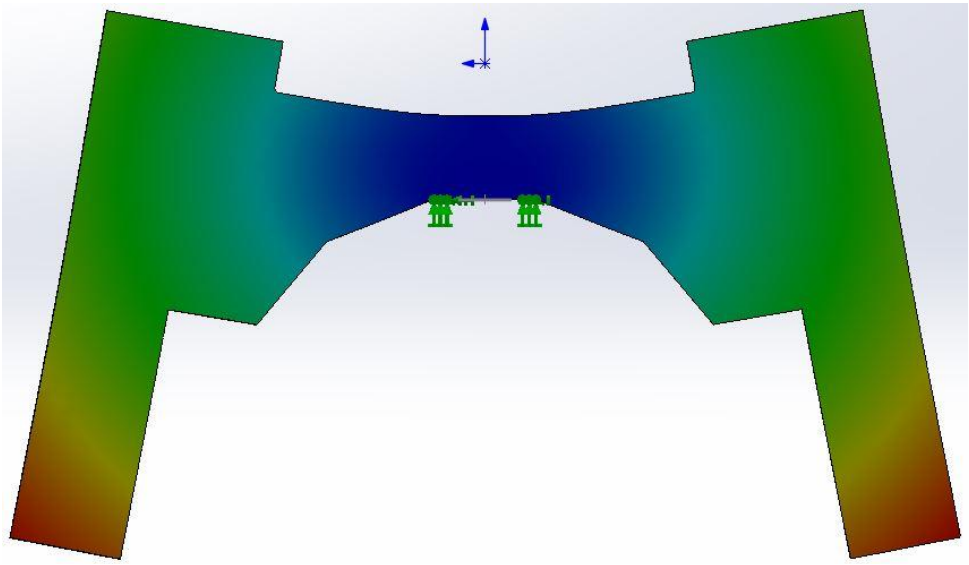

FIGURE 55: SECOND MODE OF VIBRATION

When the support is excited vertically by the mechanical shaker, the support bends upward and downward compressing and extending the fibre. In such way, the interrogator records a perfect sinusoidal signal.

6.3.2 Resonance frequency test

This test was carried out in a different way if compared with the previous one: starting from a low frequency sinusoidal motion the frequency has been gradually increased until the optical fibre clearly shows its first mode of vibration. While through SmartSoft is possible to appreciate the arise of the resonance watching the FFT plug in that shows the real time Fourier analysis. Indeed, when the resonance of the fibre arises, on the Fourier spectrum is possible to notice a clear second peak at the double of the frequency imposed by the function generator (figure 57).

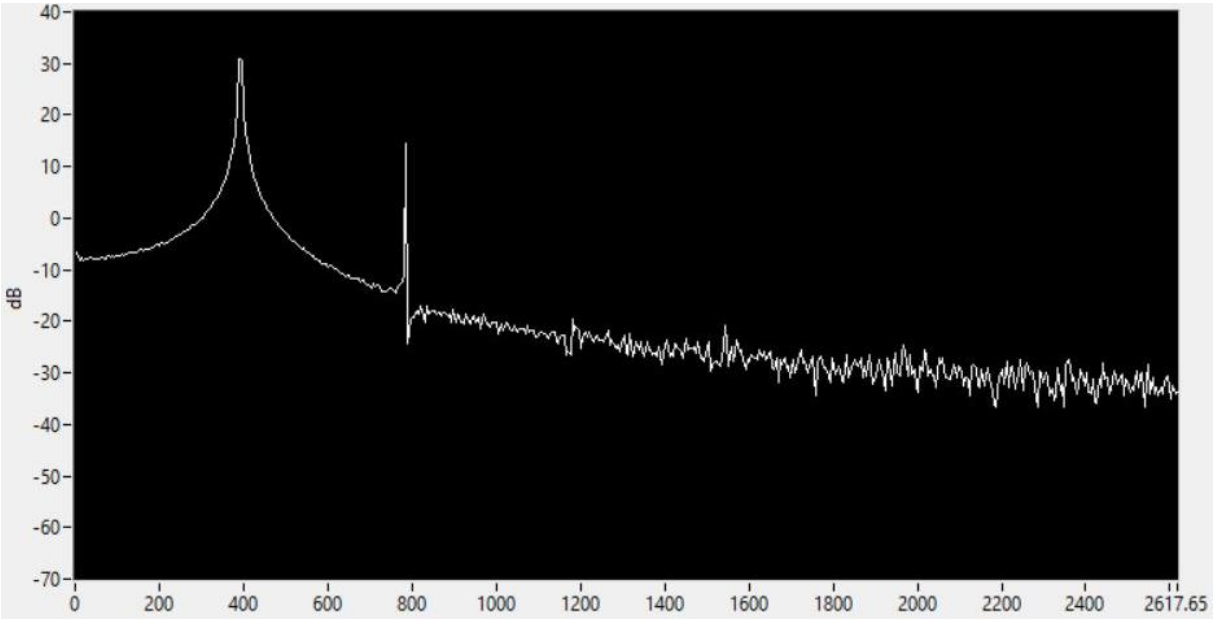

FIGURE 56: THE SECOND PEAK IS CLEARLY VISIBLE AT DOUBLE FREQUENCY

This is motivated by the fact that when the fibre vibrates with its first mode, it completes two cycles of expansion-contraction. This experimental evaluation leads us to find the natural frequency of the fibre of about 400 Hz which is slightly lower than the theoretical estimation of 600 Hz. However, this decreasing in the natural frequency was predicted because of the cap installation which complies a compression along the fibre due to the physical interference.
In figure 58 are shown the graph plotted by Matlab, while in the figure 59 is shown the fibre vibrating with its first mode.

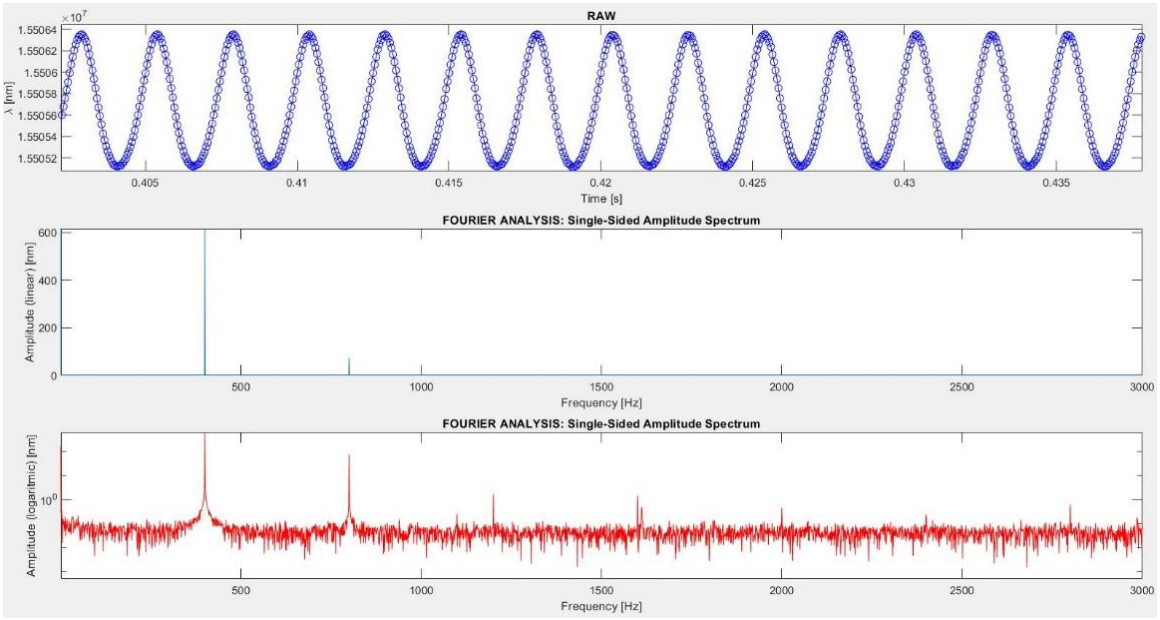

FIGURE 58: MATLAB PLOTS FOR THE RESONANCE TEST

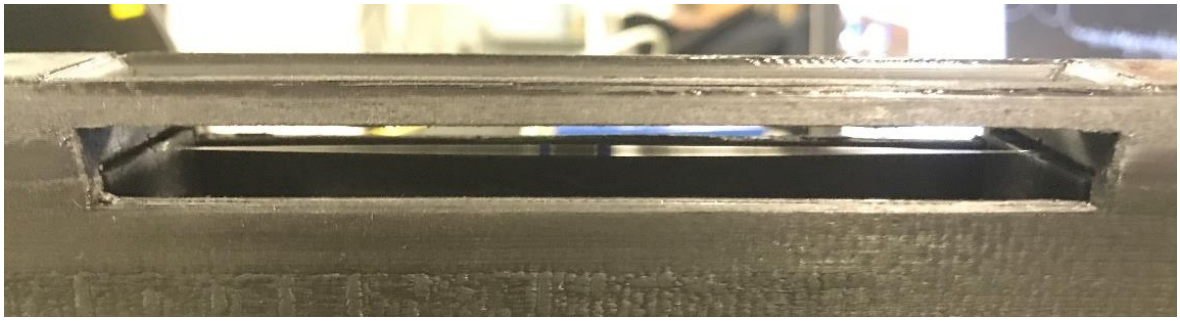

FIGURE 59: FIBRE VIBRATING WITH ITS FIRST MODE

As already known, a vibrating string can present different modes of vibration which occur at increasing frequencies and present different displacement shapes, as can be seen in figure 60.

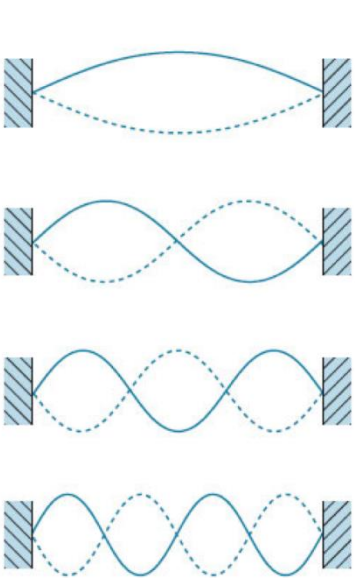

mode	wavelength	frequency
first	$2L$	$\frac{v}{2L}$
second	L	$\frac{v}{L}$
third	$\frac{2L}{3}$	$\frac{3v}{2L}$
fourth	$\frac{L}{2}$	$\frac{2v}{L}$

FIGURE 60: DIFFERENT MODES OF STRING VIBRATION

For our purposes only the first mode is relevant because it occurs at relatively low frequencies while the higher modes present at much higher frequencies.

6.3.3 SolidWorks Dynamic Simulation

In this chapter is shown a linear dynamic simulation carried out with the software SolidWorks 2019 in order to obtain a complete study of the operative conditions of the sensor mounted on the mechanical shaker [10]. The aim of the study is to know in advance when to expect some amplifications on the FBG measurements caused by the resonance of the oscillating support.
For the first part of the simulation it has been defined the material of the support (ABS, the most similar to PLA) and the constraint conditions on the lower face where the screw has been glued to. The next step of the analysis was the mesh creation (figure 61) in which have been created 14218 nodes.

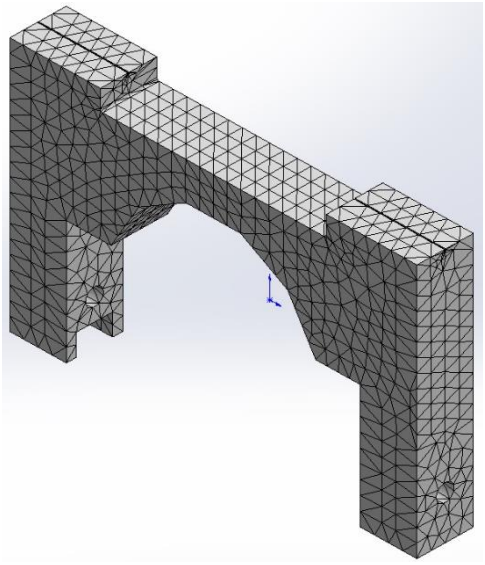

FIGURE 61: MESH

The first result is the list of the first natural frequencies of the support and the relative modes of vibration (figure 62) and, as already mentioned, the one on which the study was concentrated is the second mode which occurs at 270.95 Hz.

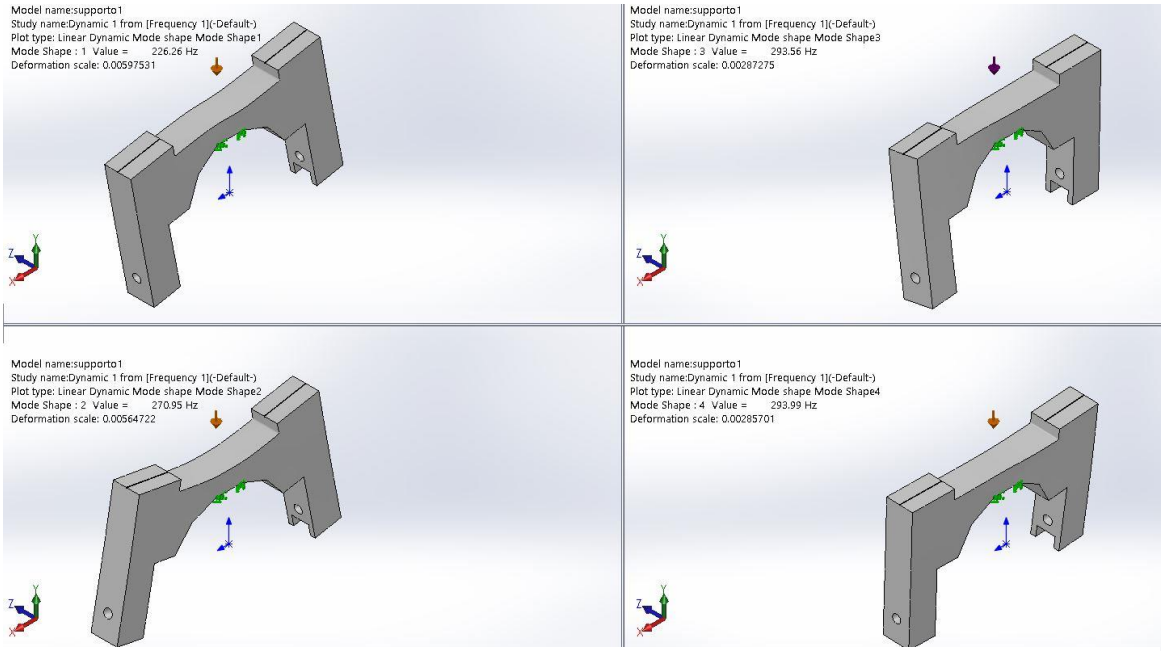

FIGURE 62: FIRST FOUR MODES OF VIBRATION

In the second part of the simulation it has been solved the harmonic analysis in which there is also the load definition and the frequency domain in which the simulation has been carried out. The load has been defined as a "uniform base excitation" applied on the same face of the constraint with the shaker and with a constant amplitude of 40 m/s^2 in the vertical direction. The frequency domain has been set from 0 Hz to 10000 Hz, in these conditions, the simulation is very consistent with the real case.
In figure 63 is reported the resultant displacement plot of the second mode in which the maximum value reached correspond to 3.944 mm.

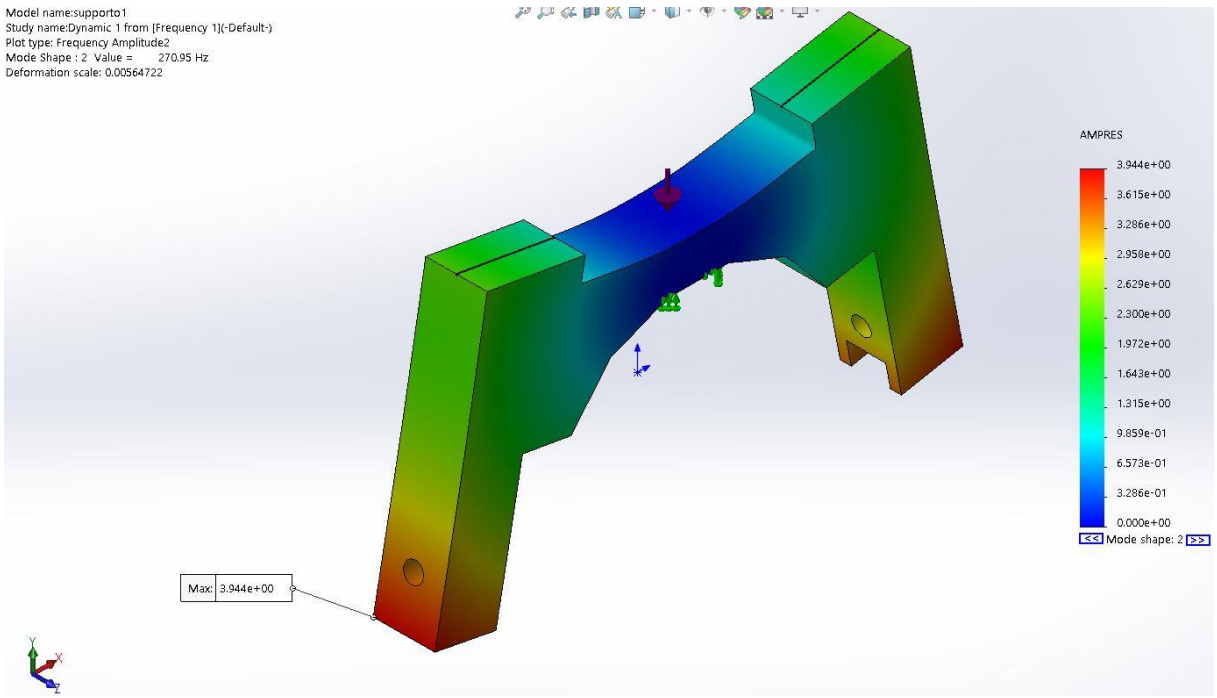

FIGURE 6357: RESULTANT DISPLACEMENT PLOT

As last result of the simulation is reported the response graph in figure 64 like a Bode diagram in which is evident the arising of the resonance around 270.95 Hz.

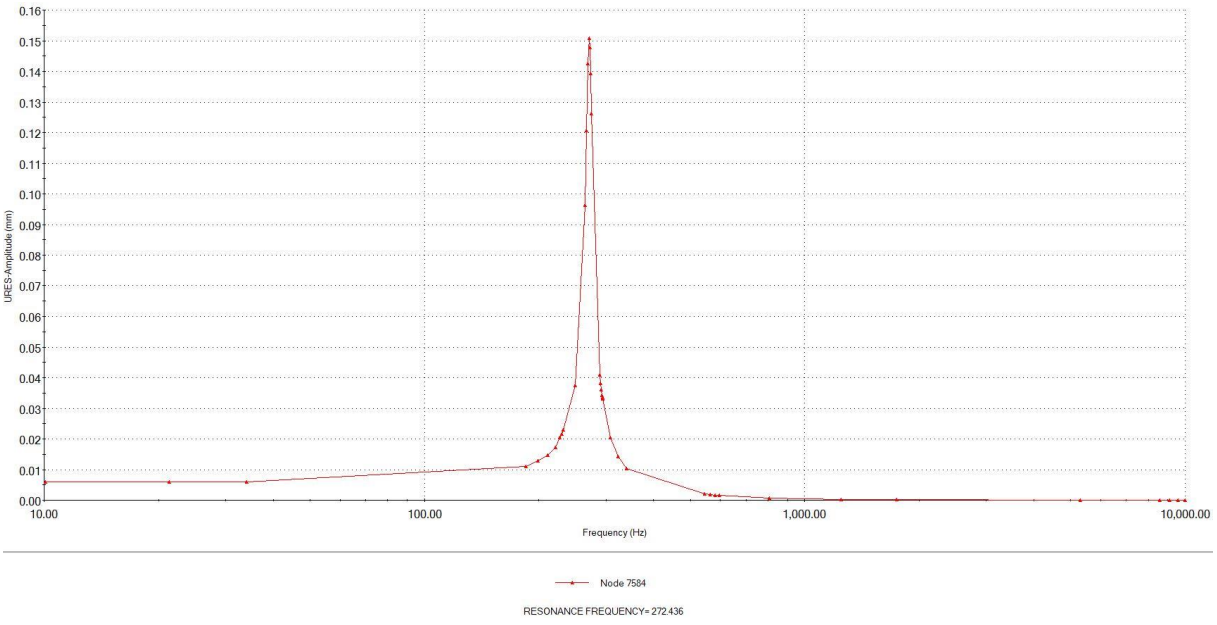

FIGURE 64: RESPONSE GRAPH

Chapter 7: Conclusions and future works

The final tests conducted with the 3D printed PLA support for the FBG showed that some of the aims of this work of thesis have been reached in the design of a vibration sensor based on Fiber Bragg Grating technology. Indeed, the tests showed how this sensor can provide information about the vibration of the body to which the support is connected and is suitable to be adopted as a regular vibration sensor.

Unfortunately, in the historical period in which this work was carried out it was marked by the arrival of the COVID-19 virus which caused many delays and program changes in the development of this thesis. In fact, both Politecnico di Torino and Scuola Camerana were closed to the students during the period in which most of the practical tests and the installation of the sensor on the test bench should have been carried out.

However, even if the optical sensor has not been tested on the vibration test bench of Scuola Camerana di Torino, the tests highlighted that it is operative to measure a wide range of frequency vibrations and it is ready to be tested on the rotating shaft.

So, hopefully this thesis will be useful for the future students which will study this topic: I have supplied the most relevant guidelines to operate both the electric motor of the test bench and the CMS vibration monitoring system.

Moreover, it has been designed, printed and tested an FBG support tailored for the bearing support of the shaft end.

In the future, it is advisable to develop a more detailed dynamic simulation in which it is needed to specify the correct fixings and excitations to which the support will be subjected and the correct mechanical characteristics of the PLA that are not contained in the solidworks library.

Obviously, it will be necessary to finally test the FBG support on the vibration test bench and compare the measurements with those obtained from the CMS monitoring system.

Bibliography

[1] Condition Monitoring systems, SM1281 Condition Monitoring Operating Instructions, 2016.

[2] G. Baima, Design and Development of a Test Bench for Frequency Analysis of FBGs Optic Sensors for Prognostic Techniques for Aerospace Applications, Tesi di laurea magistrale Politecnico di Torino, 2019.

[3] G. Candiano, Fiber Bragg Grating Sensors for Mechanical and Thermal Prognostics and Diagnostics for Aerospace Applications, Tesi di laurea magistrale Politecnico di Torino, 2018.

[4] M. Salvo, Fibre di vetro e fibre ottiche, Lecture notes, 2017.

[5] G. Spampinato, Innovative optical sensors for prognostic techniques in the aerospace field: design and development of a test bench for studying the frequency response of FBG sensors. Tesi di laurea magistrale Politecnico di Torino, 2019.

[6] A. Coscia, Manuale d'uso in riferimento all'interrogatore "SmartScan", 2018.

[7] Siemens SINAMICS V-ASSISTANT user manual, Siemens Corp, 2016.

[8] Vibration diagnostics by means of frequency analysis with a Condition Monitoring System, Siemens Industry Online Support, 2019.

[9] Master's Degree Thesis, “Optical sensors for prognostics in aerospace applications: design and development of FBG based vibration sensors”, Alessio Laudani, December 2019.

[10] Dynamic analysis, [online]. Available: https://help.solidworks.com/2019/english/SolidWorks/cworks/c_dynamic_analysis_overview.htm